



Spectroscopy[®]

Solutions for Materials Analysis

July 2013 Volume 28 Number 7

www.spectroscopyonline.com

Vis–NIR Spectroscopy and Least Squares Support Vector Machines for Apple Analysis

**X-ray Fluorescence Spectroscopy:
The Essentials**

**Femtosecond Pulse Shaping and
2D IR Spectroscopy**

**Hydrogen–Deuterium Exchange
Mass Spectrometry**

Lowest cost elemental analysis

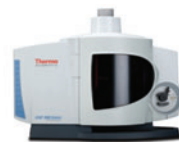
Thermo Scientific™ trace elemental instruments give you the lowest cost of analysis and the highest quality data with innovative software and award winning hardware design. Remove the hidden costs in your lab and get fast, accurate results using the iCE™ 3000 Series AA, the **NEW iCAP™ 7000 Series ICP-OES**, the iCAP™ Q ICP-MS, the Element 2™ ICP-MS and Element XR™ HR-ICP MS.

highest quality data

• [discover lowest cost analysis](#) • thermoscientific.com/iCAP7000



iCE 3000 Series AA
Easy, low cost, flame and furnace AA technology.



iCAP 7000 Series ICP-OES
Advanced performance, high productivity and lowest cost per sample.



iCAP Q ICP-MS
Breakthrough design for outstanding results and reliability.




ELEMENT2 HR-ICP-MS
High resolution ICP-MS for the most demanding applications and indisputable results.

the REMARKABLY BETTER

ATOMIC SPECTROSCOPY

RUNS on AIR

revolution



Introducing the NEW Agilent 4100 MP-AES. Say goodbye to flammable and expensive gases. Say hello to enhanced productivity. The Agilent 4100 Microwave Plasma-Atomic Emission Spectrometer runs entirely on air. It's safer and more cost efficient. It enables superior detection and unattended multi-element analysis. It's the most significant advancement in atomic spectroscopy in decades. In other words: **It's time to run on air.**

JOIN THE REVOLUTION. Learn more about the NEW Agilent 4100 MP-AES.
www.agilent.com/chem/RunsOnAir

© Agilent Technologies, Inc. 2011

The Measure of Confidence



Agilent Technologies

Spectroscopy®

MANUSCRIPTS: To discuss possible article topics or obtain manuscript preparation guidelines, contact the editorial director at: (732) 346-3020, e-mail: lbush@advanstar.com. Publishers assume no responsibility for safety of artwork, photographs, or manuscripts. Every caution is taken to ensure accuracy, but publishers cannot accept responsibility for the information supplied herein or for any opinion expressed.

SUBSCRIPTIONS: For subscription information: *Spectroscopy*, P.O. Box 6196, Duluth, MN 55806-6196; (888) 527-7008, 7:00 a.m. to 6:00 p.m. CST. Outside the U.S., +1-218-740-6477. Delivery of *Spectroscopy* outside the U.S. is 3–14 days after printing. Single-copy price: U.S., \$10.00 + \$7.00 postage and handling (\$17.00 total); Canada and Mexico, \$12.00 + \$7.00 postage and handling (\$19.00 total); Other international, \$15.00 + \$7.00 postage and handling (\$22.00 total).

CHANGE OF ADDRESS: Send change of address to *Spectroscopy*, P.O. Box 6196, Duluth, MN 55806-6196; provide old mailing label as well as new address; include ZIP or postal code. Allow 4–6 weeks for change. Alternately, go to the following URL for address changes or subscription renewal: <https://advanstar.replycentral.com/?PID=581>

RETURN ALL UNDELIVERABLE CANADIAN ADDRESSES TO: IMEX Global Solutions, P.O. Box 25542, London, ON N6C 6B2, CANADA. PUBLICATIONS MAIL AGREEMENT No.40612608

REPRINT SERVICES: Reprints of all articles in this issue and past issues are available (500 minimum). Call 877-652-5295 ext. 121 or e-mail bkolb@wrightsmedia.com. Outside US, UK, direct dial: 281-419-5725. Ext. 121

DIRECT LIST RENTAL: Contact Tamara Phillips, (440) 891-2773; e-mail: tphillips@advanstar.com

INTERNATIONAL LICENSING: Maureen Cannon, (440) 891-2742, fax: (440) 891-2650; e-mail: mcannon@advanstar.com.



©2013 Advanstar Communications Inc. All rights reserved. No part of this publication may be reproduced or transmitted in any form or by any means, electronic or mechanical including by photocopy, recording, or information storage and retrieval without permission in writing from the publisher. Authorization to photocopy items for internal/educational or personal use, or the internal/educational or personal use of specific clients is granted by Advanstar Communications Inc. for libraries and other users registered with the Copyright Clearance Center, 222 Rosewood Dr. Danvers, MA 01923, 978-750-8400 fax 978-646-8700 or visit <http://www.copyright.com> online. For uses beyond those listed above, please direct your written request to Permission Dept. fax 440-756-5255 or email: mcannon@advanstar.com.

Advanstar Communications Inc. provides certain customer contact data (such as customers' names, addresses, phone numbers, and e-mail addresses) to third parties who wish to promote relevant products, services, and other opportunities that may be of interest to you. If you do not want Advanstar Communications Inc. to make your contact information available to third parties for marketing purposes, simply call toll-free 866-529-2922 between the hours of 7:30 a.m. and 5 p.m. CST and a customer service representative will assist you in removing your name from Advanstar's lists. Outside the U.S., please phone 218-740-6477.

Spectroscopy does not verify any claims or other information appearing in any of the advertisements contained in the publication, and cannot take responsibility for any losses or other damages incurred by readers in reliance of such content.

Spectroscopy welcomes unsolicited articles, manuscripts, photographs, illustrations and other materials but cannot be held responsible for their safekeeping or return.

To subscribe, call toll-free 888-527-7008. Outside the U.S. call 218-740-6477.

Advanstar Communications Inc. (www.advanstar.com) is a leading worldwide media company providing integrated marketing solutions for the Fashion, Life Sciences and Powersports industries. Advanstar serves business professionals and consumers in these industries with its portfolio of 91 events, 67 publications and directories, 150 electronic publications and Web sites, as well as educational and direct marketing products and services. Market leading brands and a commitment to delivering innovative, quality products and services enables Advanstar to "Connect Our Customers With Theirs." Advanstar has approximately 1000 employees and currently operates from multiple offices in North America and Europe.

PUBLISHING & SALES

485F US Highway One South, Suite 100, Iselin, NJ 08830
(732) 596-0276, Fax: (732) 647-1235

Michael J. Tessalone

Science Group Publisher, mtessalone@advanstar.com

Edward Fantuzzi

Publisher, efantuzzi@advanstar.com

Stephanie Shaffer

East Coast Sales Manager, sshaffer@advanstar.com
(508) 481-5885

EDITORIAL

Laura Bush

Editorial Director, lbush@advanstar.com

Megan Evans

Managing Editor, mevans@advanstar.com

Stephen A. Brown

Group Technical Editor, sbrown@advanstar.com

Cindy Delonas

Associate Editor, cdelonas@advanstar.com

Dan Ward

Art Director, dward@media.advanstar.com

Russell Pratt

Vice President Sales, rpratt@advanstar.com

Anne Young

Marketing Manager, ayoung@advanstar.com

Tamara Phillips

Direct List Rentals, tphillips@advanstar.com

Wright's Media

Reprints, bkolb@wrightsmedia.com

Maureen Cannon

Permissions, mcannon@advanstar.com

Jesse Singer

Production Manager, jsinger@media.advanstar.com

Jason McConnell

Audience Development Manager, jmcconnell@advanstar.com

Gail Mantay

Audience Development Assistant Manager, gmantay@advanstar.com



Joe Loggia

Chief Executive Officer

Tom Florio

Chief Executive Officer Fashion Group, Executive Vice-President

Tom Ehardt

Executive Vice-President, Chief Administrative Officer & Chief Financial Officer

Georgiann DeCenzo

Executive Vice-President

Chris DeMoulin

Executive Vice-President

Ron Wall

Executive Vice-President

Rebecca Evangelou

Executive Vice-President, Business Systems

Tracy Harris

Sr Vice-President

Francis Heid

Vice-President, Media Operations

Michael Bernstein

Vice-President, Legal

J Vaughn

Vice-President, Electronic Information Technology

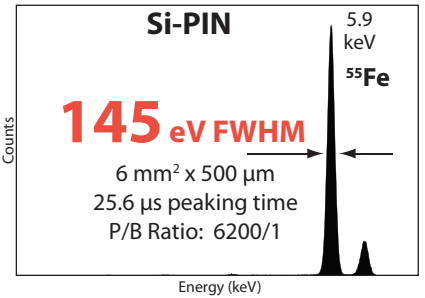
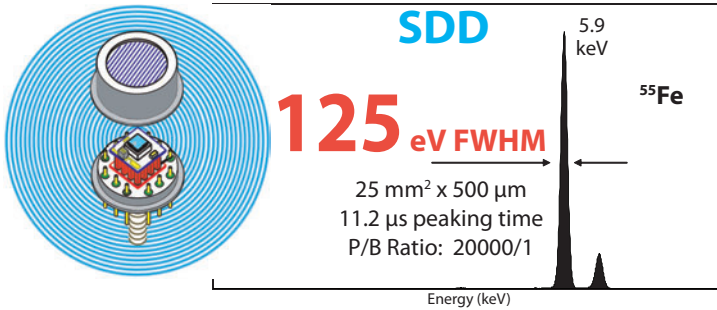
X-Ray Detectors

• Solid-State-Design

• Low Cost

• Easy to Use

The PERFORMANCE You Need



NEW!!!

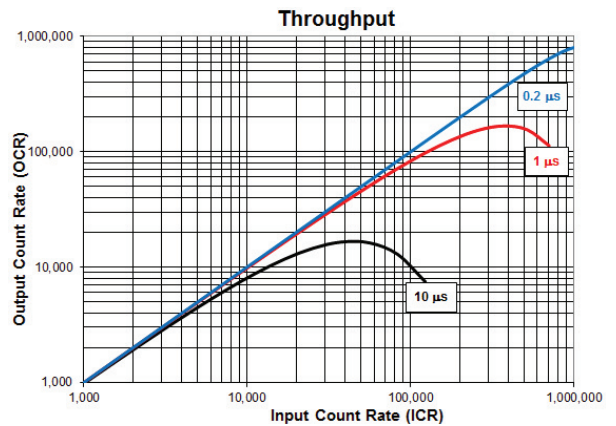
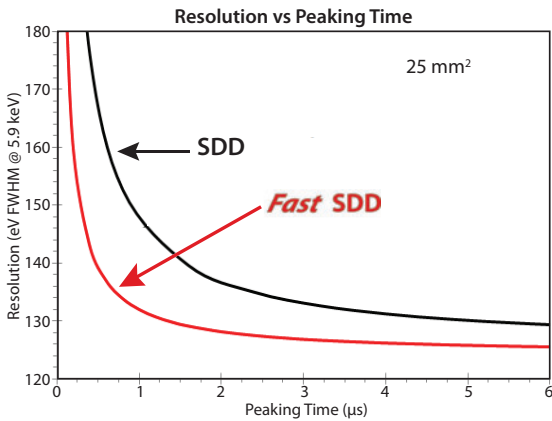
Fast SDD

NEW!!!

Count Rate = >1,000,000 CPS

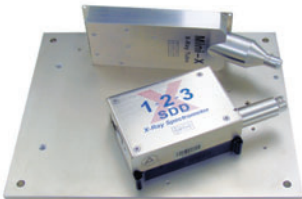
10 Times the Throughput - No Resolution Loss

Resolution	125 eV FWHM	135 eV FWHM	155 eV FWHM
Peaking Time	8 µs	1 µs	0.2 µs



The CONFIGURATION You Want

XRF Experimenter's Kit



X-Ray Spectrometer



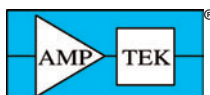
OEM Components for XRF



XRF System



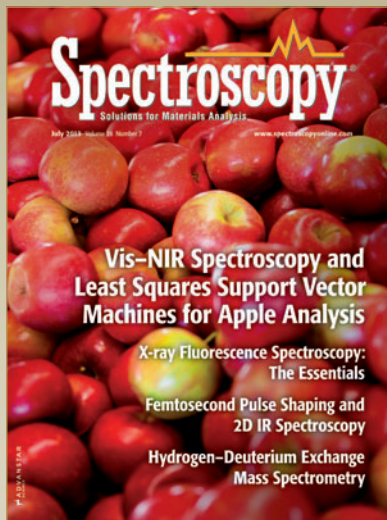
**OEM's #1 Choice
for XRF**



AMPTEK Inc.
www.amptek.com



Spectroscopy

July 2013
Volume 28 Number 7Cover image courtesy of
Archi Trujillo/Getty Images.

ON THE WEB

WEB SEMINARS

Improved Evaporation and Concentration for Better Chromatographic Analysis

James Hannan and Julian Wills,
Thermo Fisher Scientific

USP <232> and <233>: Practical Considerations for Compliance with the New Requirements on Elemental Impurities

Tim Cuff and Kevin Kingston, PerkinElmer,
and Nathan Saetveit, Elemental Scientific

Raman Spectroscopy of Oil Shale

David Tuschel, Horiba North America

Avoid the 483 – Unconventional Approaches to Elevate Your Quality Program

Michael Fricke, PhD,
Ben Venue Laboratoriesspectroscopyonline.com/webseminarsLike Spectroscopy on Facebook:
www.facebook.com/SpectroscopyMagazineFollow Spectroscopy on Twitter:
<https://twitter.com/spectroscopyMag>Join the Spectroscopy Group on LinkedIn
<http://linkd.in/SpecGroup>

CONTENTS

COLUMNS

Mass Spectrometry Forum 10

Hydrogen-Deuterium Exchange Mass Spectrometry

A detailed look at H-D exchange mass spectrometry including the history of the technique, the exchange process itself, and how the current state of the art provides insights into complex protein structures and their dynamics through the study of the rates of exchange under various conditions.

Kenneth L. Busch

Atomic Perspectives 16

X-ray Fluorescence Spectroscopy, Part I: The Educational Essentials

The main areas of training necessary for a good foundation in the analytical methodology of XRF spectroscopy are discussed.

John A. Anzelmo, Mathieu Bouchard, and Marie-Ève Provencher

Lasers and Optics Interface 24

Femtosecond Pulse Shaping Enables Rapid Two-Dimensional Infrared Spectroscopy

Martin Zanni and his group in the Department of Chemistry at the University of Wisconsin-Madison are specialists in a new class of infrared spectroscopy: two dimensional (2D) infrared spectroscopy. Here, he explains the technique, the role of lasers, and current applications, such as studying the kinetics of protein aggregation in diabetes.

Laura Bush

PEER-REVIEWED ARTICLES

Quantification of the Soluble Solids Content of Intact Apples by Vis-NIR Transmittance Spectroscopy and the LS-SVM Method 32

The feasibility of quantifying the soluble solids content of intact apples was investigated by visible and near infrared (vis-NIR) transmittance spectroscopy combined with the least squares support vector machines (LS-SVM) method.

Yande Liu and Yanrui Zhou

CONFERENCE PREVIEW

Denver X-ray Conference: 62nd Annual Conference on Applications of X-ray Analysis 44

A brief preview of what to expect at this year's Denver X-ray conference, taking place August 5-9 in Westminster, Colorado.

Megan Evans

DEPARTMENTS

News Spectrum 9 Product Resources . . . 46 Ad Index 50

Spectroscopy (ISSN 0887-6703 [print], ISSN 1939-1900 [digital]) is published monthly by Advanstar Communications, Inc., 131 West First Street, Duluth, MN 55802-2065. *Spectroscopy* is distributed free of charge to users and specifiers of spectroscopic equipment in the United States. *Spectroscopy* is available on a paid subscription basis to nonqualified readers at the rate of: U.S. and possessions: 1 year (12 issues), \$74.95; 2 years (24 issues), \$134.50. Canada/Mexico: 1 year, \$95; 2 years, \$150. International: 1 year (12 issues), \$140; 2 years (24 issues), \$250. Periodicals postage paid at Duluth, MN 55806 and at additional mailing offices. POSTMASTER: Send address changes to *Spectroscopy*, P.O. Box 6196, Duluth, MN 55806-6196. PUBLICATIONS MAIL AGREEMENT NO. 40612608. Return Undeliverable Canadian Addresses to: IMEX Global Solutions, P. O. Box 25542, London, ON N6C 6B2, CANADA. Canadian GST number: R-124213133RT001. Printed in the U.S.A.



MAGNUM® X-ray Source



XPIN-BT® Detector



CONSIDER US
PART OF YOUR
EXPLORATION
TEAM

Moxtek's® x-ray sources and detectors are **durable** and **lightweight**, making them the best solution for portable and benchtop **XRF instrumentation**.

The combination of XPIN® detector and MAGNUM® X-ray source enables high precision measurements in challenging applications, such as light element analysis, alloy sorting, or food and soil contamination detection.

- Dependable performance
- Robust design
- Simple mounting for easy integration
- Lightweight, compact, low power

For more information, please contact a sales representative at www.moxtek.com, or at info@moxtek.com.

452 West 1260 North / Orem, UT 84057 USA / Call: 1.801.225.0930 / Toll Free: 1.800.758.3110

Visit us at www.moxtek.com / ISO 9001:2008



Editorial Advisory Board

Fran Adar Horiba Jobin Yvon

Ramon M. Barnes University of Massachusetts

Matthieu Baudelet University of Central Florida

Paul N. Bourassa Blue Moon Inc.

Michael S. Bradley Thermo Fisher Scientific

Deborah Bradshaw Consultant

Kenneth L. Busch Wyvern Associates

Ashok L. Cholli Polnox Corporation

David M. Coleman Wayne State University

David Lankin University of Illinois at Chicago,
College of Pharmacy

Barbara S. Larsen DuPont Central Research
and Development

Ian R. Lewis Kaiser Optical Systems

Rachael R. Ogorzalek Loo University of California Los Angeles,
David Geffen School of Medicine

Howard Mark Mark Electronics

R.D. McDowall McDowall Consulting

Gary McGeorge Bristol-Myers Squibb

Linda Baine McGown Rensselaer Polytechnic Institute

Robert G. Messerschmidt Rare Light, Inc.

Francis M. Mirabella Jr. Mirabella Practical Consulting
Solutions, Inc.

John Monti Montgomery College

Michael L. Myrick University of South Carolina

John W. Olesik The Ohio State University

Jim Rydzak GlaxoSmithKline

Jerome Workman Jr. Unity Scientific

Contributing Editors:

Fran Adar Horiba Jobin Yvon

David W. Ball Cleveland State University

Kenneth L. Busch Wyvern Associates

Howard Mark Mark Electronics

Volker Thomsen Consultant

Jerome Workman Jr. Unity Scientific

Spectroscopy's Editorial Advisory Board is a group of distinguished individuals assembled to help the publication fulfill its editorial mission to promote the effective use of spectroscopic technology as a practical research and measurement tool. With recognized expertise in a wide range of technique and application areas, board members perform a range of functions, such as reviewing manuscripts, suggesting authors and topics for coverage, and providing the editor with general direction and feedback. We are indebted to these scientists for their contributions to the publication and to the spectroscopy community as a whole.

When do you see a Specialist?

When you absolutely need
the best...

- Technical expertise
- Quality
- Reliability
- Service



The ICP sample introduction
specialists.

Request our catalog.

Telephone: 508 563 1800
Toll Free: 800 208 0097
Email: geusa@geicp.com
Web: www.geicp.com



News Spectrum

Mike Bradley Joins *Spectroscopy's* Editorial Advisory Board

Spectroscopy is pleased to announce the addition of Mike Bradley to its editorial advisory board.

Bradley graduated from the University of South Carolina (Columbia, South Carolina) with a BS in Chemistry and earned his PhD from the University of Illinois (Urbana-Champaign, Illinois). He is the marketing manager for Fourier transform infrared (FT-IR) spectroscopy at Thermo Fisher Scientific in Madison, Wisconsin. He taught at the University of Connecticut (Storrs, Connecticut) and Valparaiso University (Valparaiso, Indiana) for a combined 15 years, and worked at Abbott Laboratories before becoming a field applications scientist with (then) Thermo Nicolet in 2002.

Bradley was heavily involved in the development and launch of the Thermo Scientific Nicolet iS10 FT-IR spectrometer and the Nicolet iN10 FT-IR microscope in 2008. He has been product manager for the FT-IR products since 2009. Most recently,



Mike Bradley

Bradley led the teams that developed the Thermo Scientific Nicolet iS50 FT-IR spectrometer, launched in 2012, and was recently promoted to marketing manager for FT-IR microscopy products.

Bruker and 3M Sign Exclusive Patent License Agreement

Bruker Corporation (Bremen, Germany) has signed an exclusive patent license agreement with 3M Company (Elyria, Ohio), which allows Bruker to use 3M patented innovations relating to matrix-assisted laser desorption-ionization (MALDI) mass spectrometry imaging.

The licensed 3M patents are directed to a technique for performing mass spectrometry analysis on proteins in tissue that has been preserved in paraffin. The technology enables researchers to more easily study formalin-fixed, paraffin-embedded tissue for life-science research and drug development.

MALDI imaging has been increasingly used to analyze clinically relevant tissues, such as tumor biopsies. The molecular phenotypes observed by MALDI imaging have been shown to correlate with parameters such as disease status or patient outcome and have been successfully applied to the classification of tissue samples. ■

Market Profile: Infrared Microscopy and Imaging

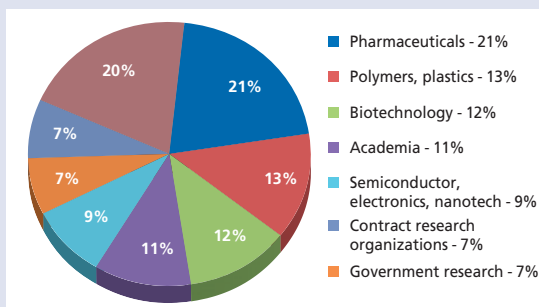
Infrared (IR) microscopy includes both conventional microscope systems and more advanced imaging systems, which are used in two ways. The more traditional IR microscopy method is “point and shoot,” where the microscope is used to locate a defect or point of interest on a sample, which is then analyzed using the IR spectrometer. Such systems are useful across a broad range of industries, such as semiconductors and electronics, pharmaceuticals, forensics, biology, and materials. IR imaging systems have all the capabilities of traditional IR microscopes, but also provide high-resolution mapping of samples by collecting IR spectral information for each pixel, which can be as small as 10 μm, or even smaller with some of the latest instruments.

The market for IR spectroscopy was more than \$150 million in 2012, accounting for close to a

quarter of the overall infrared spectroscopy market. This includes stand-alone integrated IR microscopes and imaging systems, add-on IR microscopy systems that are sold separately from benchtop spectrometers, and initial system sales that include

both spectrometer and microscope systems as a packaged solution. Although growth in demand is likely to be flat in 2013 due in large part to government funding cuts, it should rebound by late 2014, and will continue to be a driving factor of the growth of the overall infrared spectroscopy market.

The foregoing data were extracted from SDi's market analysis and perspectives report entitled *The Global Assessment Report*, 12th Edition: *The Laboratory Life Science and Analytical Instrument Industry*, October 2012. For more information, visit www.strategic-directions.com.



Infrared microscopy demand by industry for 2012.



Mass Spectrometry Forum

Hydrogen–Deuterium Exchange Mass Spectrometry

Mass spectrometric measurements often begin with the determination of the masses of ions, assuming that these are set and stable. But we can also monitor the progress of mass shifts purposefully created in our experiments, and derive reaction kinetic information. For example, labile hydrogen (H) atoms in molecular and ionic structures can be replaced with deuterium (D), and the mass shifts and kinetics can be followed as the measured ion masses progressively increase. In its current state of development, H–D exchange mass spectrometry provides insights into complex protein structures and their dynamics through the study of the rates of exchange under various conditions.

Kenneth L. Busch

It starts with the basics; many of us learn about hydrogen (H), deuterium (D), and tritium (T) in our first chemistry classes. Tritium is radioactive, but hydrogen and deuterium are not. The difference between hydrogen and deuterium, of course, is the presence of the neutron in the nucleus of the latter. Although the relative shift in mass between H (mass of 1.007825 Da) and D (mass of 2.014102 Da) is the largest of the isotopes, the discovery of deuterium occurred later than many other isotopes and, oddly enough, was not accomplished directly through experiments with mass spectrometers. The manuscript announcing the discovery of deuterium by Urey, Brickwedde, and Murphy (1) carries a date of December 5, 1931, and was published in early 1932 (1). What made that deuterium different was that extra particle in the nucleus. The publication “The Existence of a Neutron” by Chadwick carries a date of May 10, 1932, and was published June 1 of that year (2) following a brief announcement of results written on February 17 and published February 27, 1932 (3). Nobel prizes for these discoveries were awarded in 1934 and 1935, respectively (remember that Aston’s Nobel prize for mass spectrometry [MS] was in 1922). The extraordinary sequence of synergistic discoveries was the result of both impassioned competition and serendipity (4–6). The understanding that provided the basis for modern MS was also used in the development of atomic weapons in only a little over two decades from discovery. These bits of history should not be relegated to historical

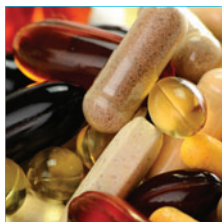
markers (Figure 1). The generation of scientists who witnessed this series of astounding discoveries has largely passed, but the processes and sometimes the serendipity of the scientific process (4) replays within each succeeding generation.

Replacing Hydrogen with Deuterium

Changes in physical parameters that occur as a result of the replacement of hydrogen with deuterium have been characterized. The *kinetic isotope effect*, which is the change in reaction rate resulting from the replacement, has been measured in many systems. New areas of applications constantly surface. For one example, deuterium-modified analogs of pharmaceutical drugs have been patented in the past five years. These analogs are being explored in the hope that improvements in the drug’s metabolic properties can be achieved. But how can we use deuterium specifically in MS, when the mass shift allows us to track hydrogen–deuterium placement in ions and ion fragments? Even within the constraints of MS, we could choose from literally thousands of applications. Two studies provide the foundation needed here. The first is the classic publication that used deuterium labeling to establish the existence of the tropylium cation (7). The mass spectra of alkylbenzenes with deuterium replacing hydrogen in specific locations, being composed of ions of different mass based on the incorporation of deuterium, were interpreted as a group to show that the seven hydrogens in the $C_7H_7^+$

Transforming Metals Prep!

NO VESSEL
CLEANING



EASY TO
USE



CHALLENGING
SAMPLES

FASTEST
RUN TIMES

UltraWAVE



MIXED
BATCHES



HIGH
THROUGH-
PUT

BENCHTOP HIGH THROUGHPUT MICROWAVE DIGESTION SYSTEM

The remarkable new UltraWAVE features Milestone's unique Single Reaction Chamber (SRC) technology in a fully automated system. Unlike closed vessel digestion, the UltraWAVE uses disposable glass vials, and different sample types can be digested simultaneously, greatly increasing productivity, and reducing overall cost per digestion.

UltraWAVE - Transforming metals sample prep!

Watch Videos, Download Brochures, Application Notes, or Request A Demo at:

milestonesci.com/ultrawave

AVAILABLE WEBCASTS:
USP <232>/<233>
&
FOOD SAMPLE PREP



PRODUCTIVITY TOOLS

digestion | clean chemistry | mercury | ashing | extraction | synthesis

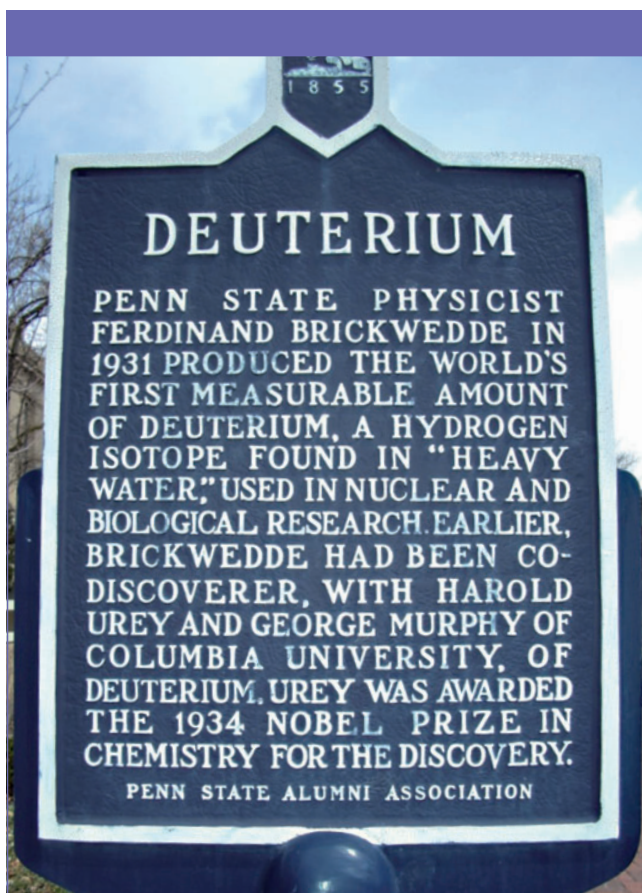


Figure 1: Marker on the campus of Pennsylvania State University that celebrates the accomplishments of physics professor F.G. Brickwedde (then at the National Institute of Standards and Technology [NIST]) in preparing samples analyzed to provide evidence supporting the discovery of deuterium. Three years after the discovery, heavy water (D_2O) was being produced on an industrial scale at a hydroelectric facility in Norway. This is one of probably only a few markers devoted to isotopes in the United States.

ion were indistinguishable, and that the ion was therefore a tropylium symmetric structure. This exemplary publication highlights the use of strategic deuterium labeling to elucidate fragmentation reactions of organic ions.

The second publication (8) built upon the uses of trimethylsilyl (TMS) derivatization. This derivatization reagent had been developed in gas chromatography (GC) and gas chromatography–mass spectrometry (GC–MS) because the derivatives were stable and volatile and the original molecules were not. The TMS group is $-Si(CH_3)_3$. As an interpretive example, the number of derivatized hydroxyl groups in a molecule could be determined because each hydroxyl hydrogen would be replaced by the TMS group, and the number of groups was therefore apparent by a simple count of the number of losses of trimethylsilanol molecules in the resultant electron ionization mass spectrum. But there are interpretive difficulties when the structure of the original molecule becomes more complicated. The use of perdeutero-TMS derivatives ($-Si(CD_3)_3$) provides information (via tracking the deuterium atoms) that helps to avoid the uncertainties. The basic mass shifts apparent in the compared mass spectra are simple: a 9-Da shift in mass rep-

resents the intact TMS group, and a 6-Da shift is the loss of a methyl (deuteriomethyl) group. Tracing the deuterium in the mass spectra of various molecules led to the deduction that rearrangement reactions reveal “the existence of coiled or wound chains in the vapor phase.” This prescient statement hints at a higher-order structure for ions that can be discerned through MS experiments.

Higher-Order Structures and Derivatization

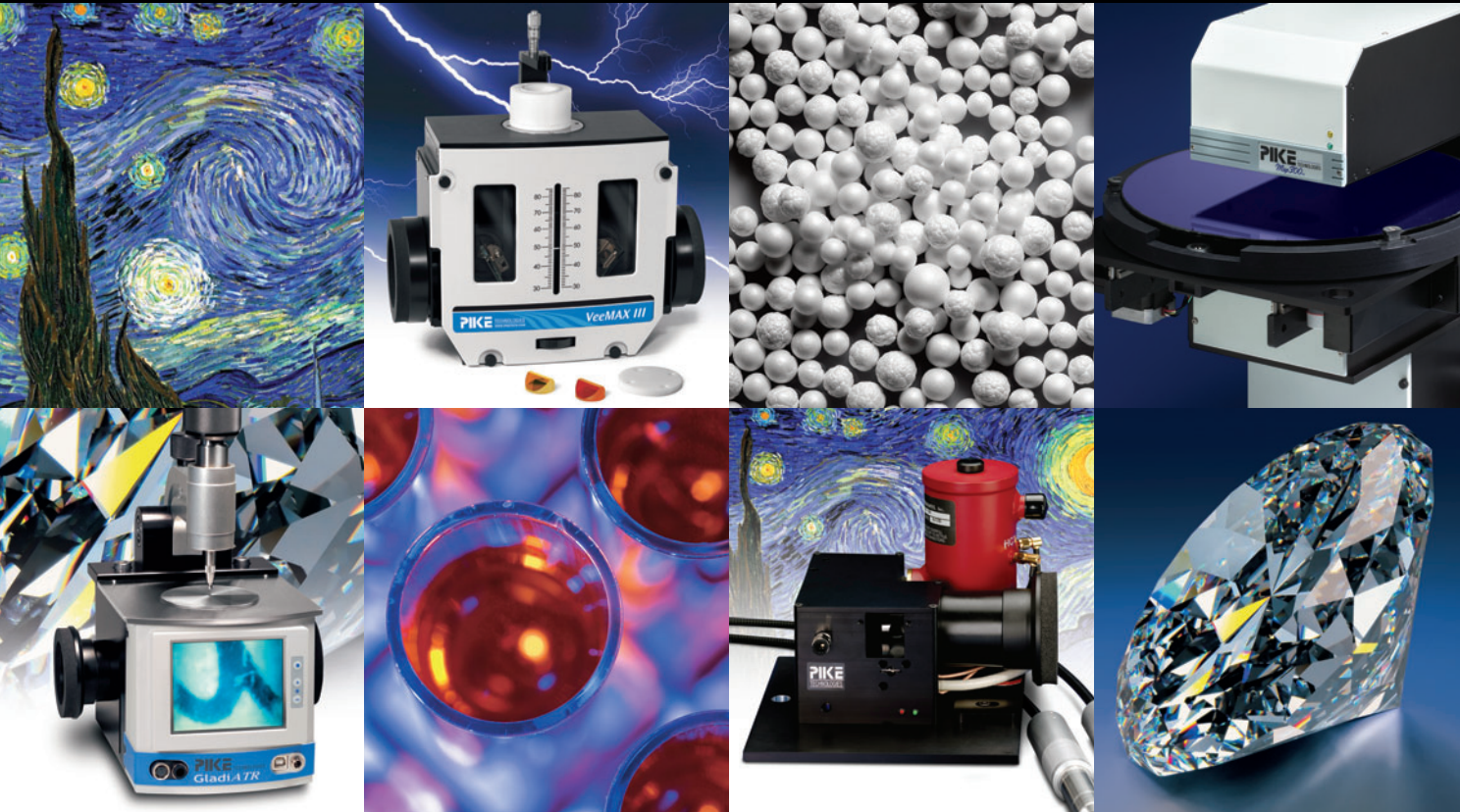
In 45 years, the study of higher-order structures and their dynamics was made possible with progressively more sophisticated analyses, and tools such as new ionization methods and ion dissociation processes. These methods couple with H–D exchange MS, and in a sense a return to the basic idea of derivatization. The derivative is the deuterium atom and the mass shift is followed with ease. Ideally, derivatization by replacement of hydrogen with deuterium does not change the intrinsic properties of the molecule, and we can discern progressively more complicated structures in both the condensed and the gas phase by tracing the deuterium. A number of reviews are available that provide background on the method, its modeling, the display and interpretation of the datasets, and the conclusions that can be drawn.

The Exchange Process

The observation that certain hydrogen atoms in proteins will exchange with deuterium when the protein is exposed to a D_2O solvent was initially established in the 1950s. Hydrogen atoms connected to the amide backbone of the protein (labile hydrogen) exchange with deuterium in buffered D_2O solvent at a varying rate depending on the accessibility of the amide bond to the solvent (9), and the dynamics of the protein structure. Hydrogen bonding, for example, within the structure itself slows the rate of exchange. Side-chain exchangeable hydrogen in residues such as Asn ($-CONH_2$), Asp ($-COOH$), Ser ($-OH$), Cys ($-SH$), or Lys ($-NH_2$) exchanges at much faster rates, again depending on location in the molecule. The exchange reactions proceed at rates that vary from fractions of a second to days. Interrogating the results at multiple points during that period provides a picture of the structure and its dynamics. Nuclear magnetic resonance (NMR) spectrometry was used to study the structures for many years. However, MS follows the mass shift that results from the exchange with great clarity, and requires less sample. The early 1990s (10,11) saw early publications that foreshadowed the potential of MS in measuring rates and in elucidating structures and their dynamics, based on the exchange of deuterium for hydrogen.

Figure 2 (top) illustrates the exchange process and its different time scales, showing the immediate exchange reactions as well as the longer term exchanges in the more inaccessible parts of the complex structure. The rates of the hydrogen exchange are determined by pH, temperature, accessibility of the region to solvent, and hydrogen bonding. The first two factors are controlled in the experiment, and the latter two are the factors that provide information about the structure of the protein. The times required for exchange may vary over as much as eight orders of magnitude, from fractions of

Spectroscopy Sampling Solutions



Whether your samples are precious or ordinary, large or small, hard or soft, liquid or solid, pure or contaminated, PIKE accessories provide ways and means for their analysis. We specialize in ATR, diffuse and specular reflectance, micro sampling, temperature control and sampling automation. We also provide custom solutions.

Contact us to order the NEW PIKE catalog (or get it on-line) for the complete picture...



FTIR, NIR and UV-Vis sampling made easier



www.piketech.com



info@piketech.com

tel: 608-274-2721

Think
PIKE
TECHNOLOGIES

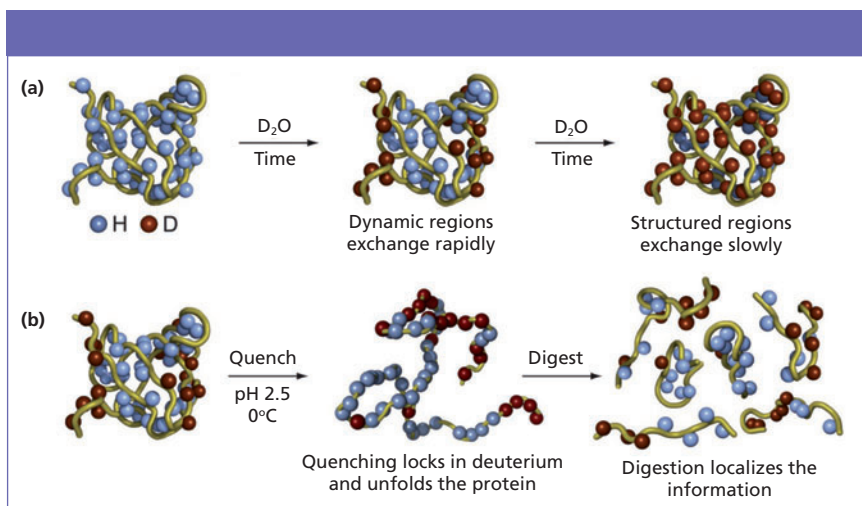


Figure 2: (a) The two exchange regimes, which are the rapid side-chain and dynamic region exchanges, and then the more slowly exchanging structured regions. (b) The exchange reactions are quenched by lowering the pH and temperature. This sample can be analyzed directly or can be digested using the usual methods into smaller peptide lengths that can be separated and analyzed. Figure adapted with permission from reference 23.

a second to days. If one were to examine molecular ions in the mass spectra at a series of times after the onset of the exchange reaction (taking out samples as a function of time, and quenching each to stop the exchange), and compare the observed masses to the ions in the unexchanged spectrum, the molecular ions for rapidly exchanged regions would display an immediate shift to higher masses. Longer-term exchanges would appear as the molecular ion masses progressed sequentially to higher values. This thought experiment is a bit more complex in reality because the molecular ions exhibit an isotopic envelope simply by virtue of their higher mass and the contributions of other isotopes. The progression to higher masses “distorts” that envelope as the exchange reactions proceed. As one simple example of data processing, the envelope can be modeled based on the known empirical formula for the ion considered. The deuterium exchange can be seen as the progressive mass spectra are compared with the immediately preceding spectra. The exchange can be monitored through the centroided mass of a group of peaks, or by dissecting each peak (including at higher mass resolving power). A common data display is called a *deuterium uptake plot*. Software to process the voluminous data generated even when

looking at only the molecular ions is widely available; below we discuss how the data production ramps rapidly upward.

Figure 2b illustrates the quenching reaction that stops the exchange reaction. Quenching usually occurs when the pH and the temperature are dropped. This change in conditions may not be perfect, and some back exchange can occur, especially for the very readily exchanged hydrogen–deuterium. The back exchange must also be considered when the sample is further processed for other mass spectral measurements. Figure 2b shows that the sample can be unfolded and then digested using relatively standard techniques. Pepsin or other proteases are used for proteolysis, and the quenched exchange must be maintained through the process. Various forms of liquid chromatography (LC) are used to separate the individual peptides, which are then analyzed by MS, often with electrospray ionization (ESI). The extent of deuterium exchange can then be established in each of the peptide fragments by comparison of mass expected and mass observed, illustrating the progressively more expansive data processing needs.

Exchange can be assessed, then, in molecular ions or in smaller parts derived from the larger structure. On reflection, it should be obvious that

the former represents the total of all exchange reactions occurring, and may not provide information relevant to specific regions of a larger structure. Probing the exchange reactivity in regions is made possible by the proteolysis illustrated in Figure 2b. Is it possible to determine the amount of deuterium exchange into individual amino acids or small chains of 2–5 amino acids? Certainly being able to assemble such information, residue by residue, over an entire structure would provide a detailed examination of its structure. The mass shift in each ion should be readily discernible, so the problem becomes how to take ionic chains of amino acids and dissociate them. Collision-induced dissociation (CID) is a mainstay of MS-MS, which has been used to sequence peptides. But it is also known that hydrogen can scramble within the ion as a result of the CID energization, rendering this specific process unsatisfactory. Studies show that electron-capture dissociation and electron-transfer dissociation can, under some conditions, provide the requisite dissociation without scrambling. The extent of H–D exchange can then be probed residue by residue. For proteins containing hundreds or thousands of residues, the management of the data can become a complex problem. Insights into how to process and interpret this data are continually being developed and refined (12,13).

Conclusions

Reviews over the past 10 years reflect the development of the method, but also different perspectives as it engages the attention of other research communities. Topics covered in the reviews include mathematical modeling of the kinetics, the display and interpretation of the datasets, new approaches and challenges, including automated workflows and the incorporation of microfluidics, and finally, the breadth and meaning of the conclusions (15–19). The method is described in general science articles (20) and even a few videos can be found online (21). The information available from H–D exchange MS extends to studies of changes in protein structure as the result of binding to an inhibitor,

protein–protein interactions, and folding and unfolding dynamics. All of this information is revealed in the plots of deuterium uptake with time for the protein as a whole, and for its subregions. Nothing in MS stays simple for long, and H–D exchange MS is a perfect example of a simple concept amplified through insightful experiments that is now being used by a broad range of scientific research and application communities. As this column was being prepared, the obituary for Virgil Woods appeared in the *Journal of the American Society for Mass Spectrometry* (22). Dr. Woods was involved in the automation of H–D exchange MS dating back to 2000. As in much of mass spectrometry today, the capabilities that we sometimes take for granted today can be traced directly to the insight, capabilities, and persistence of earlier researchers.

References

- (1) H.C. Urey, F.G. Brickwedde, and G.M. Murphy, *Phys. Rev.* **39**, 164–165 (1932).
- (2) J. Chadwick, *Proc. R. Soc. London*, **136**, 692–708 (1932).
- (3) J. Chadwick, *Nature* **129**, 312 (February 27, 1932).
- (4) F.G. Brickwedde, *Phys. Today* **35**(9), 34–39 (1982).
- (5) N. Feather, *Contemp. Phys.* **15**(6), 565–572 (1974).
- (6) J. Reader and C.W. Clark, *Phys. Today* **66**(3), 44–49 (2013).
- (7) P.N. Rylander, S. Meyerson, and H.M. Grubb, *J. Amer. Chem. Soc.* **79**, 842–846 (1957).
- (8) J.A. McCloskey, R.N. Stillwell, and A.M. Lawson, *Anal. Chem.* **40**, 233–236 (1968).
- (9) S.W. Englander and N.R. Kallenbach, *Quart. Rev. Biophys.* **16**, 521–655 (1983).
- (10) V. Katta and B.T. Chait, *Rapid Commun. Mass Spectrom.* **5**(4), 214–217 (1991).
- (11) G. Thévenon-Emeric, J. Kozłowski, Z. Zhang, and D.L. Smith, *Anal. Chem.* **64**, 2456–2458 (1992).
- (12) D.D. Weis, T.E. Wales, J.R. Engen, M. Hotchko, and L.F. Ten Eyck, *J. Amer. Soc. Mass Spectrom.* **17**, 1498–1509 (2006).
- (13) J. Zhang, P. Ramachandran, R. Kumar, and M.L. Gross, *J. Amer. Soc. Mass Spectrom.* **24**, 450–453 (2013).
- (14) J.D. Venable, W. Scuba, and A. Brick, *J. Amer. Soc. Mass Spectrom.* **24**, 642–645 (2013).
- (15) J. Engen and D.H. Smith, *Anal. Chem.* **73**, 256A–265A (2001).
- (16) T. Wales and J. Engen, *Mass Spectrom. Rev.* **25**, 158–170 (2006).
- (17) D.D. Weis, S. Kaveti, Y. Wu, and J.R. Engen, "Probing protein interactions using hydrogen-deuterium exchange mass spectrometry," in *Mass Spectrometry of Protein Interactions*, K.M. Downard, Ed. (John Wiley and Sons, Hoboken, New Jersey, 2007), pp. 45–62.
- (18) X. Yan and C.S. Maier, *Meth. Molec. Biol.* **492**, 255–171 (2009).
- (19) L. Konermann, J. Pan, and Y.H. Liu, *Chem. Soc. Rev.* **40**, 1224–1234 (2011).
- (20) <http://cen.acs.org/articles/90/i17/Easing-Toil-Hydrogen-Exchange.html>.
- (21) <http://www.jove.com/video/3602/amide-hydrogendeuterium-exchange-maldi-tof-mass-spectrometry-analysis>; <http://www.scivee.tv/node/6576>.
- (22) Y. Hamuro, *J. Amer. Soc. Mass Spectrom.* **24**, 650–651 (2013).
- (23) <http://mvsc.ku.edu/content/hydrogen-deuterium-exchange-mass-spectrometry>.



Kenneth L. Busch

at a theoretical body mass of 70 kg (<http://chemistry.about.com/od/lecturenoteslab1/a/Elemental-Composition-Of-The-Human-Body-By-Mass.htm>), contains about 7 kg of hydrogen. With a mass abundance for deuterium of 0.0312%, he therefore contains about 2.184 g of deuterium. Since all deuterium is thought to be originally formed in the Big Bang, the presence of these multibillion-year-old atoms can be invoked to explain his grey hair and cantankerous nature. This column is the sole responsibility of the author, who can be reached at wvynassoc@yahoo.com.

For more information on this topic, please visit our homepage at: www.spectroscopyonline.com



**Systems smart
enough
to help you
spot a fake**

At EDAX, we understand how you see the world. Our **Orbis Micro-XRF Analyzer** is designed to make your life easier. New SDD option improves trace element sensitivity, allows 40% faster data collection. Optional chamber viewport lets you feel secure analyzing even your most precious artifacts. Easy. Fast. Flexible.

Power your next insight with EDAX.

AMETEK
MATERIALS ANALYSIS DIVISION

edax.com

EDAX
Smart Insight



Atomic Perspectives

X-ray Fluorescence Spectroscopy, Part I: The Educational Essentials

This column installment is the first in a series describing the educational components and processes necessary in learning the technique of X-ray fluorescence (XRF) spectroscopy. Here, we discuss the main areas of training necessary for a good foundation in the analytical methodology of XRF spectroscopy. The installment begins with the place of XRF in the analytical instrumentation spectrum and defines its capabilities and compares them to other elemental analysis techniques. Then a description of a general spectrometer is provided so that the different types and capabilities of the various XRF spectrometers can be listed and understood. This leads to a discussion of the conceptual physics that occurs during XRF analysis, including the physics of the interactions occurring inside the sample that are not related to the spectrometer.

John A. Anzelmo, Mathieu Bouchard, and Marie-Ève Provencher

After one goes through the process of evaluating different types of X-ray fluorescence (XRF) spectrometers, and then purchases one, the next task is learning how to use it. Operation of the instrument has now been reduced to pushing one button for production laboratory operation with the vendor initially supplying the program setup and calibration necessary to facilitate this method of analysis for the main bread and butter operations of the laboratory. However, when a new material appears on the task list, and the operator must build a program and calibrate the XRF system by themselves, that is when the fun starts. It soon becomes clear that a basic foundation of X-ray physics, as well as some knowledge of how to build a “general application,” will be necessary to prepare the instrument to give the most accurate and precise analysis possible and to have confidence in the analysis should it be challenged.

There are not as many resources for acquiring an education in XRF as one might think if the goal is to build a solid foundation of concepts and experience in the necessary areas of X-ray physics, instrumentation hardware, XRF (vendor specific) software, and applications knowledge (Figure 1). Many good texts are available from experts in the field (1–3) and articles about the subject give good guidance (4,5), but

slogging through them is not desirable in the high productivity, “little time to do things” world of today. Manufacturers normally provide customer user courses, but from necessity they must focus on the particular hardware components of their instrument, which vary from vendor to vendor, and on the operation of their particular software, which even varies from model to model within a manufacturer’s product line. This leaves little time for the fundamental X-ray principles and even less time for suggesting generalities between applications: Many concepts can be taught about “Element X,” rather than speaking about a specific element. In fact, the typical beginner is frustrated by the discussion of “Element X,” desiring to speak about the specific elements dealt with in his or her everyday operations instead. Eventually, however, as certain general concepts are applied and practiced, the advantages of learning this way become apparent. Ultimately, all parties concerned realize that there is a lot to learn and that it will take a long time to learn it well. To do so, many basic concepts must be taught first, as is so with any scientific endeavor based on physics, mathematics, and chemistry.

So, the hope of the vendors is to give enough training in the typical one-week course to allow the attendee to return to his or her laboratory and produce results with a new XRF

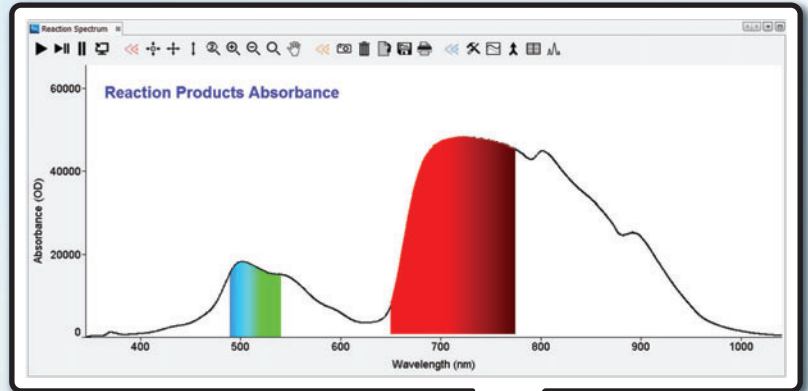


New OceanView Software

from Ocean Optics

A Simple and Powerful Solution for Your Lab

Acquire and visualize your data easily, customize data processing using schematic view, and visualize your results in the form of an answer, rather than just a simple waveform.



Get Your **FREE**
10-Day Trial at
oceanoptics.com



SPECTROMETERS | ACCESSORIES | SUB-SYSTEMS | COMPLETE SOLUTIONS



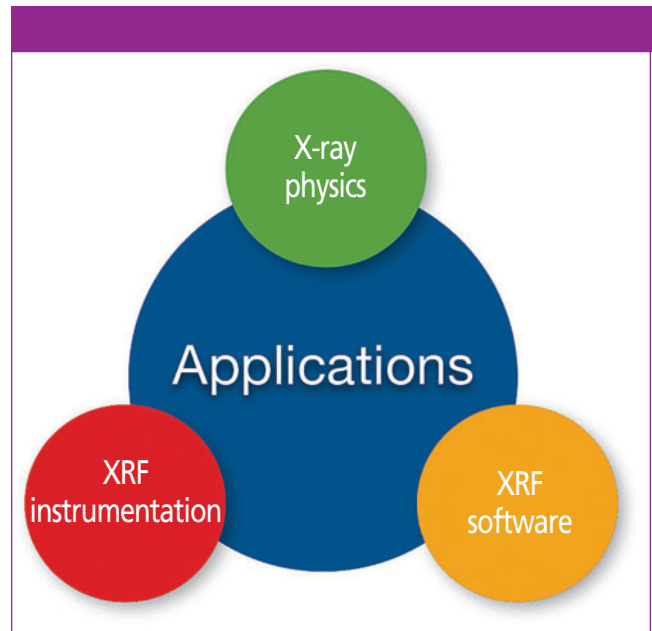
www.oceanoptics.com
info@oceanoptics.com
+1 727-733-2447



Table I: Elemental analysis by XRF

Environmentally clean and safe
Simple and fast sample preparation
Can be nondestructive
Qualitative, semiquantitative, and quantitative analysis
Standardless analysis
X-ray spectra less complex than other techniques
All elements from Na to U in any kind of sample
Relative precision of 0.1% easily obtained
Concentrations ranging from sub-ppm to 100%

system. Having been in this situation for the better part of 27 years with X-ray manufacturers, and having been responsible for customer training for most of that time, this author (J.A.A.) can vouch for this description of the teaching and learning process with confidence. This is an unfortunate situation for which there is no alternative in the industrial world. Furthermore, the study of the XRF discipline is so rich and varied, that it is only after a great deal of study, application, and trial and error, that one begins to accumulate enough knowledge to accelerate the process of learning. Therefore, after a student acquires a certain amount of knowledge regarding his or her specific hardware and software, it is possible and hoped for that the user can or will now “bootstrap” himself along. Often, this results in uncer-

**Figure 1:** XRF education foundation.

tainty about how to develop a new method and uncertainty about the numbers that are produced when using it. In the United States, a course has been designed to expand the user's knowledge into the areas of the fundamental physics and general applications, thus allowing a more confident approach to setting up a new specific application and trusting the numbers it generates (6).

The Place of XRF in the Grand Unified Theory of Physics — The Electromagnetic Spectrum

It is useful to first determine the place of the X-ray technique in the overall world of physics and chemistry. We start with the *grand unified theory* (GUT) of physics (as good a place as any to start), which describes the universe in terms of the four fundamental forces of nature (the strong nuclear force, the weak nuclear force, the electromagnetic spectrum, and gravity). Now we can narrow our discussion to the electromagnetic spectrum (Figure 2). Nature provides a continuous range of wavelengths (or energies) on which many instrumental techniques are based. As can be seen, the X-ray region occupies an area of high energy and short wavelengths, which range approximately from 0.01 to 20 nm. It is important to note the inverse relationship between wavelength and energy. This phenomenon can cause many a problem during the initial learning period if not understood and remembered.

X-ray Capabilities

Before going further, it is necessary to make sure the choice of instrumental technique will solve the analytical task at hand. Because XRF is blessed with many unique capabilities (Table I), it has become the technique of choice for many applications requiring accurate elemental analysis for the purpose of meeting tight specifications at high concentration levels. These

High-Resolution High-Stability Spectrometers

from \$1,559/ea*



- Superb temperature & long-term stability
- High spectral resolution (sub-nm)
- High throughput, with SMA fiber input
- USB2.0 for both data and power
- Trigger input and 4-pin GPIOs
- Interchangeable slits (5~200µm)
- Full-featured SDK

*Better performance
Lower prices*



Multi-Channel CCD Spectrometer



- Multiple (6) individual spectrometer channels in one compact package
- No moving parts
- USB2.0 for both data and power
- External trigger and GPIO's
- Full-featured SDK for OEM

*Simultaneous measurement
of multiple spectra*



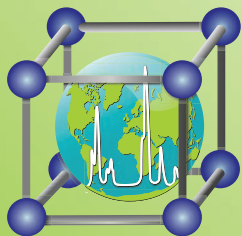
* For US shipping addresses only.

Order Online, Ship Worldwide, Free Tech Support

Simply Brighter
Mightex

Tel.: (USA) +1-925-218-1885
(Canada) +1-416-840-4991
email: sales@mightex.com

www.mightex.com or www.mightexsystems.com



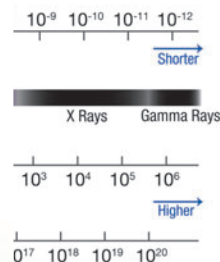
International Centre for Diffraction Data

PDF-4⁺ 2013

Identify and Quantitate

The PDF-4+ database is ICDD's most advanced database, designed for both phase identification and quantitative analysis. For quantitative analysis the database has the following features:

- ❖ All 340,653 entries have digital patterns for use in total pattern analysis
- ❖ 243,065 entries have I/I_c values for quantitative analysis by Reference Intensity Ratio
- ❖ 227,102 entries have access to atomic coordinates for quantitative analysis by Rietveld method
- ❖ 8,032 entries have experimental digital patterns
- ❖ Digital reference patterns for noncrystalline materials



Material	Materials
Aluminum	Inorganics
Aluminum Oxide	Inorganics
Aluminum Hydroxide	Inorganics
Aluminum Nitrate	Inorganics
Aluminum Chloride	Organics
Aluminum Sulfate	Organics

accurate analyses are obtained using analytical lines that are free of line overlap. An example of the simplicity of the XRF spectra is shown in Figure 3. The analytical lines most commonly used for XRF analysis are the K-alpha and K-beta lines. There are only five other iron lines that might possibly be used for analysis, but usually they are not. In fact, eight is the highest number of lines that can be used for analysis for the highest atomic numbered elements. In contrast, the spark emission lines for iron are shown in Figure 4. This spectrum, like those of many of the elements analyzed using other spectroscopic techniques, has thousands of lines, making the choice of line to be analyzed very difficult, and matrix dependent. The difficulty can be imagined from a multicomponent matrix containing many elements, all of which generate thousands of lines. Keeping this in mind, a review of the capabilities of some of the most common instrumental techniques for elemental analysis (Table II) will narrow the analyst's choice quickly to the best instrument for the task at hand.

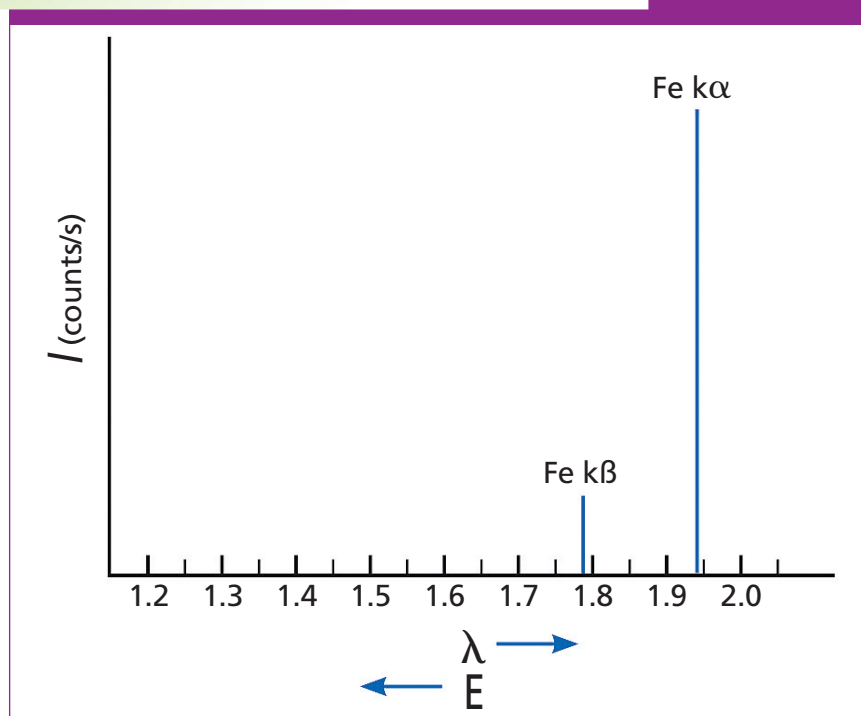


Figure 3: XRF emission lines of iron.

XRF Instrument Configurations

The next concept to be understood when learning and choosing the XRF technique is the spectrometer configuration type. Most hardware configurations

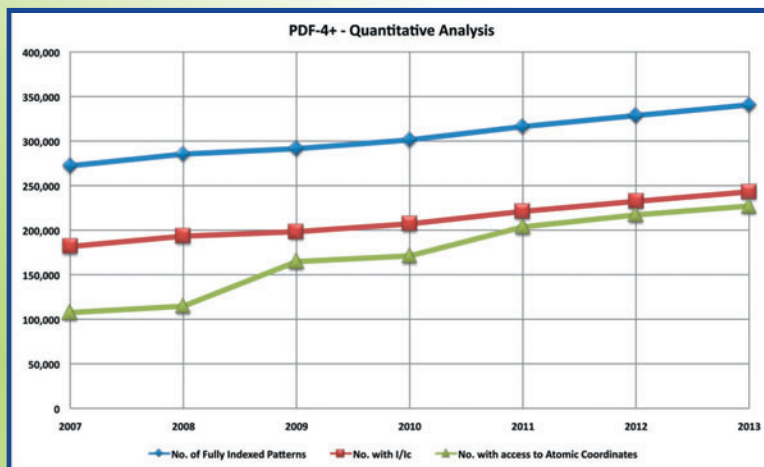
of XRF instrumentation are relegated to either wavelength-dispersive XRF (WDXRF or just WDX), and energy-dispersive XRF (EDXRF or just EDX). Figures 5 and 6 show the different

Table I: Elemental analysis

Environmentally clean
Simple and fast sample
Can be nondestructive
Qualitative, semiquantitative
Standardless analysis
X-ray spectra less common
All elements from Na to U
Relative precision of 0.1-1%
Concentrations ranging from

system. Having been in the industry for 27 years with X-ray microscopy, I am able to provide a reliable solution for customer training. (J.A.A.) can vouch for the learning process with this situation for which there is no world. Furthermore, the data is rich and varied, that it is a challenge to apply, and trial and error is enough knowledge to overcome. Therefore, after a student gains knowledge regarding the software, it is possible and now "bootstrap" himself

PDF-4+ contains an array of tools that supplement conventional analyses, such as a full suite of data simulation programs enabling the use of neutron, electron, or synchrotron data, in addition to X-ray data. PDF-4+ features digitized patterns, molecular graphics and atomic parameters.



For more information, contact marketing@icdd.com

International Centre for Diffraction Data

12 Campus Boulevard ♦ Newtown Square, PA 19073-3273 U.S.A.

Phone: 610.325.9814 ♦ Toll free: 866.378.9331 (U.S. & Canada only) ♦ Fax: 610.325.9823

www.icdd.com ♦ www.dxcicdd.com

ICDD, the ICDD logo and PDF are registered in the U.S. Patent and Trademark Office.

High-Resolution High-Stability Spectrometers

from \$1,559/ea*



- Superb temperature & long-term stability
- High spectral resolution (sub-nm)
- High throughput, with SMA fiber input
- USB2.0 for both data and power
- Trigger input and 4-pin GPIOs
- Interchangeable slits (5~200 μm)
- Full-featured SDK

*Better performance
Lower prices*



Multi-Channel CCD Spectrometer



- Multiple (6) individual spectrometer channels in one compact package
- No moving parts
- USB2.0 for both data and power
- External trigger and GPIO's
- Full-featured SDK for OEM

*Simultaneous measurement
of multiple spectra*



* For US shipping addresses only.

Order Online, Ship Worldwide, Free Tech Support

Simply Brighter

Mightex

www.mightex.com or www.mightexsystems.com

Tel.: (USA) +1-925-218-1885

(Canada) +1-416-840-4991

email: sales@mightex.com

and general applications, thus allowing a more confident approach to setting up a new specific application and trusting the numbers it generates (6).

The Place of XRF in the Grand Unified Theory of Physics — The Electromagnetic Spectrum

It is useful to first determine the place of the X-ray technique in the overall world of physics and chemistry. We start with the *grand unified theory* (GUT) of physics (as good a place as any to start), which describes the universe in terms of the four fundamental forces of nature (the strong nuclear force, the weak nuclear force, the electromagnetic spectrum, and gravity). Now we can narrow our discussion to the electromagnetic spectrum (Figure 2). Nature provides a continuous range of wavelengths (or energies) on which many instrumental techniques are based. As can be seen, the X-ray region occupies an area of high energy and short wavelengths, which range approximately from 0.01 to 20 nm. It is important to note the inverse relationship between wavelength and energy. This phenomenon can cause many a problem during the initial learning period if not understood and remembered.

X-ray Capabilities

Before going further, it is necessary to make sure the choice of instrumental technique will solve the analytical task at hand. Because XRF is blessed with many unique capabilities (Table I), it has become the technique of choice for many applications requiring accurate elemental analysis for the purpose of meeting tight specifications at high concentration levels. These

applications include cement, mining, geology, catalysts, oils, plastics, steel, iron, high alloys, super alloys, precious metals, nonferrous metals, ferro-alloys, and many others. The attributes that bring it to the top of the list for these applications are

- the wide range of elements it is capable of determining on a routine basis (Na through U);
- the wide range of concentrations it is capable of analyzing (parts per million to 100%);
- fast and easy sample preparation for most materials analyzed;
- the ability to achieve better precision with increasing concentration (0.1%) in very short analysis times; and
- a relatively simple spectrum that, unlike many other techniques, has relatively few analytical wavelengths from which to choose, thus providing a spectrum that is uncluttered and free of line overlaps.

Although line overlaps can be removed by a plethora of mathematical methods, the best approach and most accurate analyses are obtained using analytical lines that are free of line overlap. An example of the simplicity of the XRF spectra is shown in Figure 3. The analytical lines most commonly used for XRF analysis are the K-alpha and K-beta lines. There are only five other iron lines that might possibly be used for analysis, but usually they are not. In fact, eight is the highest number of lines that can be used for analysis for the highest atomic numbered elements. In contrast, the spark emission lines for iron are shown in Figure 4. This spectrum, like those of many of the elements analyzed using other spectroscopic techniques, has thousands of lines, making the choice of line to be analyzed very difficult, and matrix dependent. The difficulty can be imagined from a multicomponent matrix containing many elements, all of which generate thousands of lines. Keeping this in mind, a review of the capabilities of the some of the most common instrumental techniques for elemental analysis (Table II) will narrow the analyst's choice quickly to the best instrument for the task at hand.

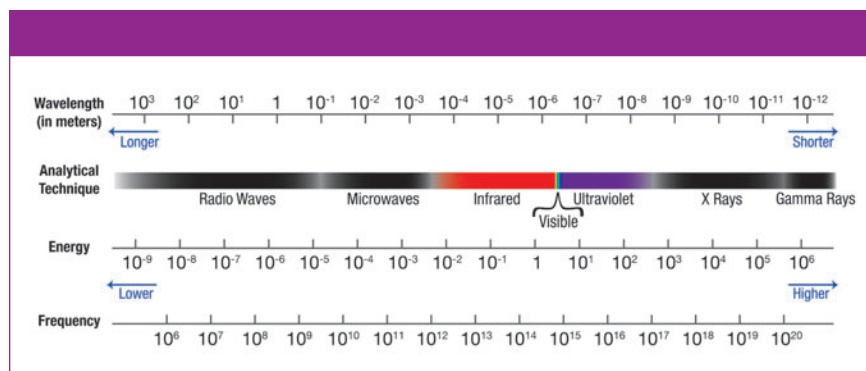


Figure 2: Electromagnetic spectrum.

Table II: Comparison of analytical techniques				
Technique	Precision	Range/Use	Sample Preparation	Materials
XRF	0.1%	ppm–100%	5–15 min	Inorganics
ICP–AA	3%	ppb–ppm	Solutions, hours to days	Inorganics
OE-spark	1%	ppm–5%	Conductive–easy	Inorganics
Neutron activation	0.5%	ppm–100%	None	Inorganics
NMR (MRI)	Qualitative	Organic–imaging	Difficult	Organics
NIR, FTIR	Qualitative	Organic–functional	Difficult	Organics

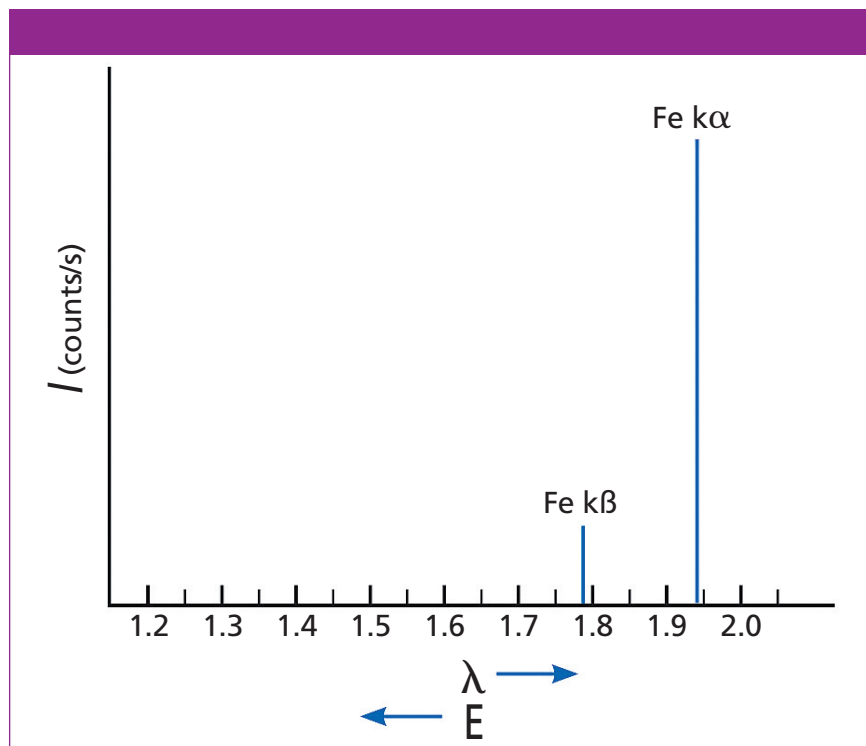


Figure 3: XRF emission lines of iron.

XRF Instrument Configurations

The next concept to be understood when learning and choosing the XRF technique is the spectrometer configuration type. Most hardware configurations

of XRF instrumentation are relegated to either wavelength-dispersive XRF (WDXRF or just WDX), and energy-dispersive XRF (EDXRF or just EDX). Figures 5 and 6 show the different



Figure 4: Spark emission lines of iron.

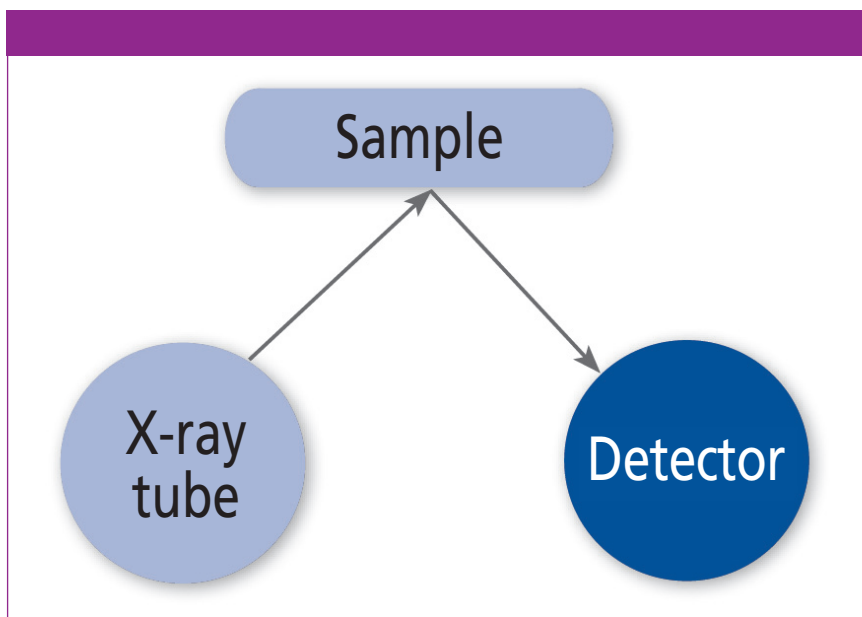


Figure 5: X-ray fluorescence spectrometers — energy-dispersive XRF (EDX, EDXRF).

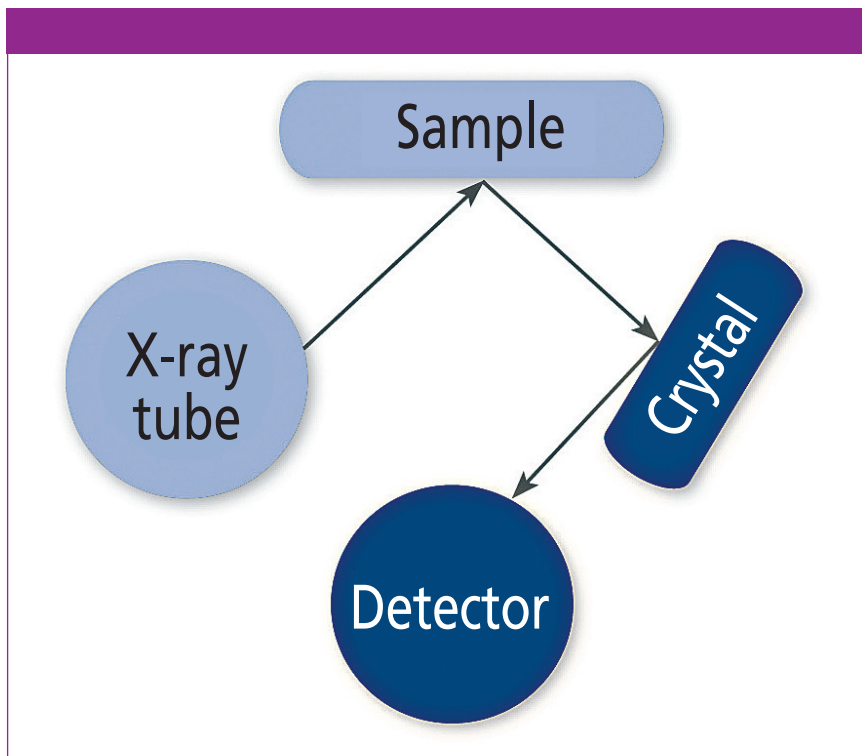


Figure 6: X-ray fluorescence spectrometers — wavelength-dispersive XRF (WDXRF).

concepts and component configurations used with these two different XRF

spectrometer types. The EDX system excites a sample using an X-ray tube,

generating characteristic radiation for each element in the sample. A portion of that radiation is directed to a detector, which serves the purpose of determining the energy of each characteristic X-ray generated (qualitative analysis) and the number of X-ray photons per second for each energy (quantitative analysis) simultaneously. A computer containing various algorithms converts the intensity (number of photons per second) for each element to concentration.

The WDXRF system operates in a similar fashion, except that an analyzing crystal is inserted between the sample and the detector for the purpose of separating (resolving) the different wavelengths (energies), and then directing those wavelengths to the detector individually, one at a time in sequence (sequential WDXRF spectrometer). These two different configurations have different advantages and disadvantages and will be discussed in a future column installment.

It is useful now to consider the concept of a “general” spectrometer (Figure 7). A modern “general” spectrometer is composed of components such as a source, a sample area, a dispersion device, a detector, processing electronics, a microprocessor, and possibly a computer and printer. Different individual sources are designed and used to generate all of the wavelengths (energies) in the electromagnetic spectrum for the various instrumental techniques and at different power levels. In the case of XRF, sealed X-ray tubes are capable of power levels ranging from 1 to 4000 W. The dispersion devices can be gratings, natural crystals, or layered synthetic microstructures. XRF uses the latter two. Detector types range from gas filled to solid state and even charge-coupled devices (CCD) for XRF. The microprocessors serve as the interface with the human operator and direct and coordinate all of the operations of the spectrometer, including capturing the data, processing it, or sending it to a computer for processing, or a network for distribution and storage. Some of the more important fundamental laws of physics that allow these components to perform their functions are listed in Table III and will be discussed in a future installment.

Choosing only the components to make an XRF system, the spectrometer can be configured for bulk analysis to support production of primary materials such as steel, high alloys, cement, catalysts, nonferrous materials, oil and fuels, and plastics. Recent XRF configurations include handheld spectrometers used for metal sorting and mining prospecting, as well as environmental and toxic metal screening. Thin-film applications, wafer fabrication processing applications, microanalysis, automated systems eliminating human interaction from sampling to delivery of analysis, and other custom, noncommercial, specialized, industrial, or proprietary “home-made” XRF system configurations that populate the industrial world have been well established for decades.

Qualitative, Quantitative, and Standardless Analysis – Data Reduction

Qualitative and Standardless Analysis
With the advent of automated elemental identification software routines, manual

Table III: Important XRF concepts	
Duane Hunt law	$\lambda_{\min} = 12.4/kV$
Moseley’s law	$1/\lambda = K(Z - \sigma)^2$
Beer-Lambert law	$I = I_0 e^{-\mu\rho t}$
Relationship between atomic number, amperage, and voltage	$I = (1.4 \times 10^{-9}) iZV^2$
Bragg’s law	$n\lambda = 2d \sin \theta$

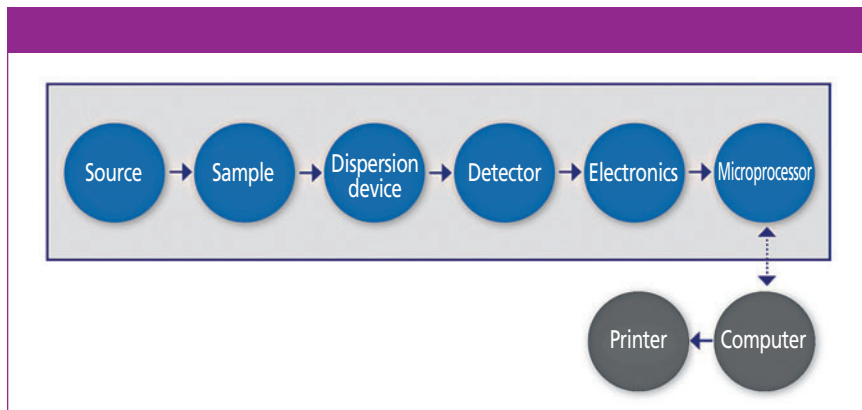


Figure 7: Concept of a general spectrometer.

identification of the elements by the operator for qualitative analysis became less and less popular. The development of capable, standardless analysis soft-

ware further hastened the decline of manual identification to the point that manual identification of the spectrum is nearly extinct. Nevertheless, the reliabil-

NEW

Benchtop sequential WDXRF spectrometer for elemental analysis of oxygen (O) through uranium (U)



Supermini200

Value — Power — Versatility



200W of power coupled with resolving power for those not uncommon overlaps



Rigaku Corporation and its Global Subsidiaries
 website: www.Rigaku.com | email: info@Rigaku.com



ity of automated identification becomes problematic below 100 ppm and human abilities begin to outperform automated software routines at that level. In many cases, it may be necessary to closely inspect an automated qualitative analysis before reporting or it may be necessary to simply perform it manually because of the complexity of the matrix. In these cases, knowledge of the basics of qualitative analysis is required and these skills are often neglected because of time restraints.

Standardless analysis has varying degrees of accuracy depending on the matrix, and it is best for the novice XRF operator to learn what those capabilities are and, in general, why they are limited. For instance, accuracies on steel over a very wide range can approach an impressive 1% relative. However, when analyzing pressed powders the error can balloon to 5%, and even 10% relative, again depending on the matrix. The implementation of the sample preparation method for different ma-

trices is paramount to the accuracy that can be achieved and, once again, this topic needs to be well understood and practiced if there will be any hope to achieve an accurate analysis. The choice between pressed powder and fusion sample preparation is quite important. The fundamental physics and chemistry of these preparation methods as well as when and when not to use them will be the topic of a future installment.

Quantitative Analysis

After the data have been processed to remove detector curvature, missing dead time counts, drift correction phenomena, and line overlap problems, the intensities (in counts per second) can be converted to weight percent concentrations by means of a calibration curve constructed from reference standards and intensities from the XRF system. Because XRF is a comparative technique, the rule of thumb is that the more the matrix of the standards is like the matrix of the unknowns, the higher the accuracy will be. For this reason, the method of preparation of both the standards and the unknowns is paramount to achieving the highest accuracy possible. After the operations described previously have been performed to acquire corrected intensities, there are several different conversion algorithms beyond straight line regression that make corrections for the interelement effects (absorption and enhancement) occurring in the sample before the characteristic intensities even get to the rest of the spectrometer. A good grasp of both mathematical and statistical concepts is necessary in choosing the appropriate algorithm for calibration to keep the operator from reporting grossly incorrect results. The theoretical process of using the fundamental parameter method of processing the data has become more and more popular and should also be learned and kept in the operator's bag of tools.

Finally, the topics of precision and accuracy, counting statistics, random and systematic error, analysis of variance, multiple regression, and limit of detection (LOD) need to be understood in terms of what they mean, and how to calculate them.

The Next Generation of NIR Spectroscopy CCD



iDus 416

Low dark-current deep-depletion (LDC-DD) technology

- Back-illuminated, deep depletion CCD with up to **95% QE**, **10x better dark current** and **fringe suppression**.
- High resolution **15 μm pixel** matrix with extended **30 mm wide array** - capture more at higher resolution.
- TE-cooling to **-95°C**, combined with Andor's **Ultravac™** platform for superior performance year after year.

Key Applications

- VIS-NIR Raman / SERS / TERS / Stimulated / SORS
- Photoluminescence
- Plasmonics
- Broadband Absorption / Reflection / Transmission
- Micro-luminescence and micro-Raman

andor.com/idus



ANDOR

Conclusions

After all of these concepts are presented, explained, discussed, and practiced, the XRF student is ready to face the real life laboratory and the challenges of producing accurate and credible numbers with the XRF spectrometer. The next installment will discuss the fundamental X-ray physics concepts taking place in the sample and the XRF spectrometer.

References

- (1) E.P. Bertin, *Principles and Practices of X-ray Spectrometric Analysis*, 2nd ed. (Plenum Press, New York, 1975).
- (2) R. Jenkins, *X-ray Fluorescence Spectrometry*, 2nd ed. (John Wiley & Sons, New York, New York, 1999).
- (3) R. Jenkins and J.L. de Vries, *Practical X-ray Spectrometry*, 2nd ed. (Springer-Verlag, New York, New York, 1969).
- (4) J.A. Anzelmo and J.A. Lindsay, *J. Chem. Educ.* **64**(8), A181–A185 (1987).
- (5) J.A. Anzelmo and A.I. Buman, "Evaluation Criteria for Wavelength Dispersive XRF Instrumentation," *American Laboratory*, International Scientific Communications, Fairfield, New Jersey, 1988.
- (6) ICDD XRF Clinic, "Practical X-ray Fluorescence," annual, Newtown Square, Pennsylvania, <http://www.icdd.com/education/xrf.htm>.



Marie-Ève Provencher is a Technical Representative (M.Sc. Chemist) with Corporation Scientifique Claisse in Quebec City, Quebec, Canada.

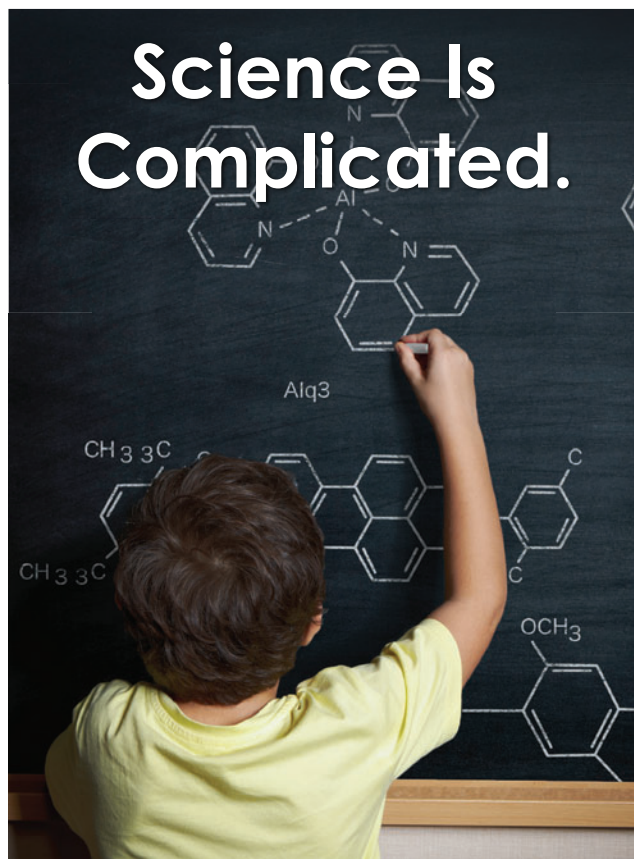


Mathieu Bouchard is the Fusion and XRF Applications Manager (M.Sc. Chemist) with Corporation Scientifique Claisse in Quebec City, Quebec, Canada.



John A. Anzelmo is the president of Claisse USA in Madison, Wisconsin. He is also the ICDD XRF Technical Program Director for the International Centre for Diffraction Data in Newtown Square, Pennsylvania.

For more information on this topic, please visit our homepage at: www.spectroscopyonline.com



Measurement Should Be Easy.



- Mercury Analyzers
- Laser Ablation
- Nebulizers
- Automation
- Sample Preparation



do more
www.cetac.com





Lasers and Optics Interface

Femtosecond Pulse Shaping Enables Rapid Two-Dimensional Infrared Spectroscopy

Martin Zanni and his group in the Department of Chemistry at the University of Wisconsin-Madison (Madison, Wisconsin) are specialists in a new class of infrared spectroscopy: two-dimensional (2D) infrared spectroscopy. To collect a 2D IR spectrum, one uses a series of infrared femtosecond laser pulses to pump and then probe the response of the system. Using this technique, it is possible to probe the structures and dynamics of molecules. In this interview, Zanni explains the technique and how it is enabled by specialized laser methods. He also discusses current applications of the technique, such as solar cell research and the study of the kinetics of protein aggregation in type 2 diabetes.

Laura Bush

What is 2D IR spectroscopy?

Zanni: Everyone knows that infrared spectroscopy is one of the most used analytical and research techniques in the world. It is often the first tool used to assess the chemical composition of a substance or the success of a reaction, because functional groups have characteristic vibrational frequencies. Students learn to interpret Fourier transform infrared (FT-IR) spectra in their undergraduate organic chemistry class. While frequencies are useful, vibrational motions of molecules contain an enormous wealth of information that goes far beyond what can be measured in an FT-IR spectrum. Vibrational coupling tells us if two molecules are bound to one another. Vibrational dynamics reveal solvation. Vibrational energy flow provides bond proximity. Vibrational transition dipoles give bond angles. Two-dimensional IR spectroscopy provides the means to extract these quantities, which are otherwise not available from an FT-IR spectrum.

Two-dimensional IR spectroscopy is the multidimensional analog of FT-IR spectroscopy. An FT-IR spectrometer measures the vibrational spectrum of a sample by probing it with an infrared pulse. In 2D IR spectroscopy, we first provide an infrared pump pulse that vibrationally excites the molecules in the sample, and then we probe the sample again, some time later. By varying the frequency of the pump pulse, we can create a 2D spectrum that correlates the vibrations that were pumped with those that were probed. The correlation occurs because the molecules are vibrationally coupled. Vibrational coupling provides information about structure, binding, and dynamics.

As an example, consider the FT-IR spectrum shown in Figure 1, which is collected for a dilute mixture of two molecules. The FT-IR spectrum contains three absorption bands. We know from the frequency range that these bands must correspond to functional groups with triple-bond character, but which functional group

HORIBA

Scientific



Mesa-50



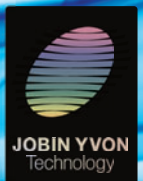
Don't Toy with the Wrong Elements!

MESA-50, the new EDXRF analyzer from **HORIBA Scientific**, helps identify hazardous elements such as Pb, Cd, Cr, Hg, Br for RoHS, ELV compliance, and Cl for halogen-free applications. MESA-50 is also useful for geology, forensics, archeology and metallurgy to name a few.

MESA-50's 5S Technology puts everything you need for EDXRF in one affordable, portable, easy-to-use analyzer. So whether you need to ensure regulatory and safety compliance, need to know that you have the right amounts of elements, or what elements are present, the MESA-50 is an affordable, convenient, easy-to-use, reliable and safe way to get the answers!

www.mesa50.com
email: adsci-specty@horiba.com

Solutions for:
Elemental Analysis
Fluorescence
Ellipsometry
Raman
OEM Spectrometry
Optical Components
Forensics
Particle Characterization



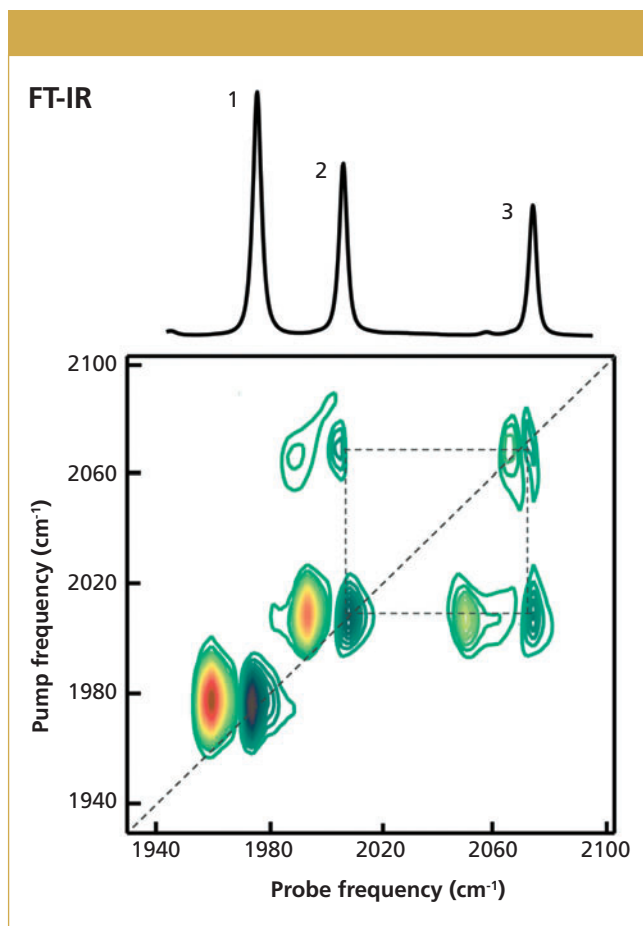


Figure 1: Experimental FT-IR and 2D IR spectra for a mixture of $W(CO)_6$ and a rhodium dicarbonyl (RDC). For each peak in the FT-IR spectrum, the 2D IR spectrum exhibits a pair of diagonal peaks. The cross peaks in the 2D IR spectrum reveal that the two higher frequency peaks are coupled to one another, which is because peaks 2 and 3 are from a rhodium dicarbonyl (RDC) whereas peak 1 is from $W(CO)_6$. $W(CO)_6$ and RDC do not have cross peaks between them because the mixture is too dilute. (Data collected by Tianqi Zhang.)

belongs to which molecule? The measured 2D IR spectrum for the same mixture is also shown. Notice that each of the absorption bands in the FT-IR spectrum produces a pair of peaks along the diagonal in the 2D IR spectrum. A diagonal slice along a 2D IR spectrum contains essentially the same information as an FT-IR spectrum. In addition, there are pairs of cross peaks between peaks 2 and 3, but not between peaks 1 and 2 or between 1 and 3. Thus, peaks 2 and 3 are vibrationally coupled, but neither is coupled to peak 1. Therefore, from the peak pattern we can quickly and confidently assign peak 1 to one molecule and peaks 2 and 3 to the other. In fact, the solution is a mixture of $W(CO)_6$ (peak 1) with a rhodium metal dicarbonyl (peaks 2 and 3). The peaks in the rhodium dicarbonyl exhibit very strong cross peaks because they share a common metal atom, but do not couple to the modes of $W(CO)_6$ because the two molecules do not bind to one another. Thus, the cross peaks show us connectivity between

absorption bands, and this information in turn teaches us about structure. Of course, mixtures like this can be disentangled using just FT-IR spectroscopy, such as by peak fitting with a spectral library or changing the concentration. But in many cases, the additional information from 2D IR spectra provides information not easily obtainable by other means. I give a few examples below in answers to other questions.

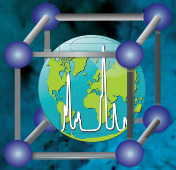
Why did you start pursuing this technique?

Zanni: Peter Hamm, Manho Lim, and Robin Hochstrasser published the first 2D IR spectrum (1) in 1998 just as I was finishing my PhD. I was thinking ahead to my postdoctoral research and was looking for an emerging research direction that had a lot of potential. I chose well. The first spectra in 1998 were rough, but with technological improvements and a better understanding of vibrations, the field has blossomed. 2D IR spectroscopy is now being used in scientific fields as diverse as materials, biophysics, and nanotechnology, as well as becoming a useful analytical tool.

What types of information can be obtained with 2D spectroscopy that cannot be obtained with one-dimensional IR?

Zanni: With FT-IR spectroscopy you are pretty much limited to absorption frequencies and pattern recognition of the fingerprint region. Two-dimensional IR spectroscopy provides information about connectivity through vibrational couplings and environment through dynamics.

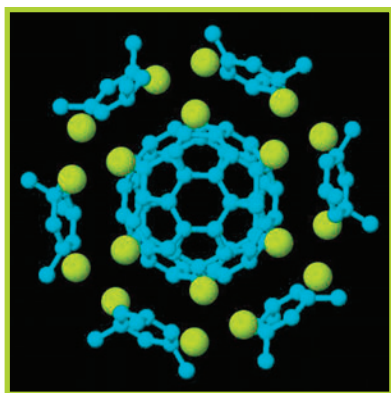
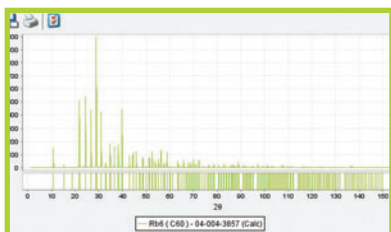
Perhaps the best way to answer this question is to provide some examples. We have studied the trans-membrane domain of the M2 proton channel from the influenza virus. The M2 channel is the binding site of amantadine, which is an anti-flu drug that has been used for 40 years. By studying the 2D lineshapes, which provide information about hydration, we were able to determine the residues that line the pore and observed a previously unknown structural change upon channel gating. We were able to determine hydration by creating a photon echo pulse sequence that measured the amount of Gaussian vs. Lorentzian lineshape that contributes to the absorption band. It turns out that Gaussian lineshapes are very sensitive to hydration but Lorentzians are not. It is very difficult to rigorously extract these components from an FT-IR spectrum. Another example is the aggregation of the human islet amyloid polypeptide (amylin). This peptide self-assembles into long fibers that are associated with type 2 diabetes. As a result, there is an enormous interest in understanding and inhibiting this fiber growth. By monitoring the coupling between strands, we were able to map the mechanism by which these proteins assemble, in what I believe is still the most detailed mechanism for any of the 20 human diseases caused by amyloids (2).



PDF-4+ 2013

***Designed for phase identification
and quantitative analysis***

***Comprehensive materials database
featuring 340,653 entries***



All entries have digital patterns for use in total pattern analysis

227,102 entries with access to atomic coordinates

243,065 entries have I/I_c values for quantitative analysis by Reference Intensity Ratio

8,032 entries have experimental digital patterns

All entries are stored in a standardized format for easy search and interpretation

All entries go through a rigorous editorial process to ensure quality

Visit us at DXC Booth 9



www.icdd.com | marketing@icdd.com
610.325.9814 | toll-free 866.378.9331



ICDD, the ICDD logo and PDF are registered in the U.S. Patent and Trademark Office.
Powder Diffraction File is a trademark of JCPDS—International Centre for Diffraction Data.



MERCURY ANALYZERS



MA-3000 Direct Mercury Analysis



- » Direct Mercury Analysis with No Sample Preparation
- » Lowest Detection Limits Available!
- » Widest Linear Range Available!
- » A Single Calibration Curve for Entire Analytical Range
- » Solids, Liquids, and Gases on One Analyzer

IS YOUR
MERCURY ANALYZER
MEETING YOUR
EXPECTATIONS?

hg-nic.us

Nippon Instruments North America
1.877.247.7241

What were the main challenges you had to overcome to make 2D IR spectroscopy work?

Zanni: The main challenge to implementing 2D IR spectroscopy is generating the pulse sequences. In many ways, 2D IR spectroscopy is analogous to 2D nuclear magnetic resonance (NMR) spectroscopy. In 2D NMR, one uses a sequence of radio frequency pulses to measure the coupling between nuclear spins. In NMR, it is quite simple to generate the pulse sequences because radio frequency technology has been around for decades. For 2D IR, most often four laser pulses are required to generate a spectrum. As you might imagine, overlapping four laser beams in space and time is very challenging even for experts in ultrafast spectroscopy, especially considering that mid-IR laser beams are invisible to the naked eye.

My research group made two contributions that helped solve this technical barrier. First, we showed that one does not need four separate beams, but that two would suffice. Using two beams also eliminates a whole bunch of other difficulties associated with producing the highest resolution spectra with the proper phasing so that positive peaks point up and negative peaks point down. Second, we invented a way of computer programming the laser pulses, so that pulse sequences can be generated with ease and on the fly, without having to rearrange optics. We can now collect spectra in seconds that used to take hours. Our approach is now being used by many research groups across the world. It simplifies the spectrometer to such an extent that my former postdoctoral researcher Dr. Chris Middleton and I have started a company together to commercialize pulse shapers and 2D IR spectrometers, which is called PhaseTech Spectroscopy, Inc.

How exactly does mid-IR pulse shaping work?

Zanni: Femtosecond pulse shaping was invented about 20 years ago to

manipulate visible laser light. There are a number of different ways of doing it in the visible, and several research groups tried to extend those methods into the mid-IR, but with limited success. One of the original ways, but possibly the most under appreciated, was by Professor Warren Warren. He used an acousto-optic modulator that filtered the spectrum of the laser light. He tailored the sound wave in the modulator with an arbitrary waveform card and thus could computer program the pulse shapes. We mimicked his approach, but used an acousto-optic modulator made of germanium so that it would work directly in the mid-IR.

Why is pulse shaping better than the other potential solutions — hole-burning and four-wave mixing?

Zanni: One of the neat things about 2D IR via pulse shaping is that you can program the pulse sequence to do whatever you want. Our pulse shapers can collect spectra using either a hole-burning or a four-wave mixing approach. In fact, hole burning done with our pulse shaper is better than with etalons (the traditional way of creating the narrow pulses), because you can use a Gaussian- instead of a Lorentzian-shaped pump pulse (which has better resolution). For any pulse sequence we can also use phase cycling, which was not previously possible, which enables a host of new capabilities including the elimination of mechanical chopping, and thus decreases data collection time by a factor of two. Regarding four-wave mixing, the original way of using four-wave mixing involved having all four pulses have independent laser beams. A setup like that could use our pulse shaper — in fact, we do something similar when collecting 3D IR spectra — but that beam geometry has all the problems associated with high resolution and phasing that I mentioned above. Since inventing our pulse shaping method, we have disassembled all of

the four-wave mixing setups in my research group.

What limitations does the pulse-shaping method have?

Zanni: The pump-probe beam geometry that the pulse shaper utilizes has been criticized for being less sensitive than a four-beam mixing geometry, but to my knowledge no one has done a quantitative comparison (I wish that I had done one before disassembling our four-wave mixing setup; rebuilding one would take months).

Polarized laser pulses are a very powerful way of probing molecular structure because they can measure the relative orientations between functional groups or can be used to eliminate diagonal peaks from the 2D IR spectra (which sometimes obscure the weaker cross peaks). The standard pulse shaper can do some, but not all polarizations. My research group has also built a polarization pulse shaper that can

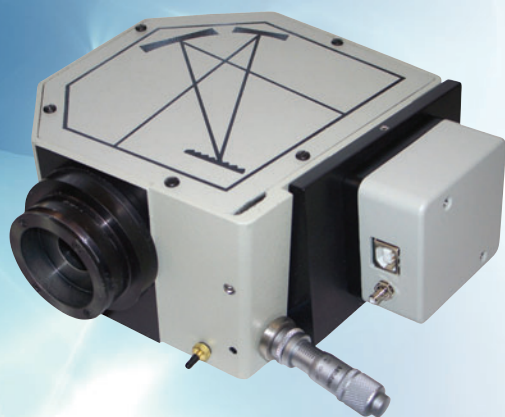
create any polarization sequence that one wants, although that style of pulse shaper is not yet available commercially through PhaseTech. Perhaps the biggest drawback is the throughput efficiency of the pulse shaper, which is about 25%. In principle this can be 40 or 50%, and improvements are being made, but it turns out that efficiency is a minor drawback. In the last few years it has become straightforward to generate 25–40 μJ of mid-IR commercial laser sources. To put that quantity in perspective, the first 2D IR experiments in 1998 were done with 1 μJ . In my opinion, the benefits of pulse shaping far outweigh the limitations. I am convinced that the productivity of my research group has surged in the past five years due to mid-IR pulse shaping.

One area where you are applying the technique of 2D IR spectroscopy is to the study of the kinetics of protein aggregation,

specifically in the study of amyloid proteins involved in type 2 diabetes. What have you been able to see that you could not have seen with other methods?

Zanni: We published a paper in *Nature Chemistry* last year that I think exemplifies the types of information that we can obtain with our approach better than other approaches (3). Amyloid fiber formation is an extremely difficult problem for X-ray crystallography and NMR spectroscopy because solving the problem requires information about both structure and kinetics. In this *Nature Chemistry* paper, we studied a model peptide inhibitor from rodents. The rodent peptide does not aggregate and so it was used to design a drug that was approved by the US Food and Drug Administration. We thought that the rodent peptide would inhibit amylin aggregation by breaking up the C-terminal beta-sheet of the fibers, and would be otherwise inert. Instead, it prevented

Oriel® LineSpec™ Spectrometers



When a Mini-spectrometer Just Won't Do!

- Up to 0.1 nm resolution
- 400:1 signal-to-noise ratio
- UV to NIR useable spectral range
- Intuitive spectroscopic application software

When a 2-D array bench top spectrometer is over budget and a mini-spectrometer just doesn't meet the requirements – consider the new LineSpec Spectrometer from Oriel. This user-configurable, linear CCD array system with 1/8 m tunable spectrograph offers superior resolution and great flexibility. Gratings and slits are interchangeable and the input can be configured for free space or fiber optic delivery.

Learn more about Oriel's new LineSpec Spectrometer today; please call 800-714-5393 or visit www.newport.com/LineSpec-8

Oriel
INSTRUMENTS
A Newport Corporation Brand

the N-terminal sheet from forming and ultimately itself templated into beta-sheet fibers onto the side of the human fibers. This rodent peptide had never before been observed to form amyloid fibers. In fact, neither of the usual methods for studying amyloid structures, TEM and ThT fluorescence, revealed any structural changes. Thus, not only were the results surprising, but it exemplified the information content available from 2D IR that is not easily obtained with other methods.

How did your method enable you to see what you saw?

Zanni: We were able to make these novel insights because of three capabilities made possible by 2D IR spectroscopy. First, just as with FT-IR spectroscopy, we can study aggregates, membrane proteins, and other systems that are not easily amenable to X-ray crystallography or NMR spectroscopy. Second, our pulse-shaping technology collects data so quickly that we can monitor kinetics on the fly. That enables us to monitor the real-time aggregation of these proteins. Third, we get good structural information. In our amyloid studies we usually also use isotope labeling, in which case we can obtain residue level structural information on a kinetically evolving system of an aggregate. In this regard there are few, if any, other comparable techniques.

What conclusions or insights are you gleaning from these results?

Zanni: One satisfying result from our work was a collaboration that was formed with James Nowick, who is an organic chemist at the University of California-Irvine. Nowick designs amyloid inhibitors. He saw my talk, and based on the mechanism, he and I designed a series of inhibitors together. They worked as we intended and we are now writing a manuscript on the topic. It illustrates that, for amyloid formation, the final fiber structure is less important for designing inhibitors than are intermediates.

Another field to which you have applied this method is solar cell research — specifically the study of charge injection, which is a key step in the conversion of solar to electrical energy in dye-sensitized nanocrystalline thin films. Why was this a good problem to tackle using your method?

Zanni: This problem is a good one for our method for similar reasons as for amyloid aggregation described above: NMR and most other standard structural tools cannot be applied to semiconductor interfaces like dyes on semiconductors. Thousands of dyes have been studied as potential next-generation solar cell materials, but the structure and orientation for nearly all of these dyes on the TiO_2 is unknown. Two-dimensional IR spectroscopy has the added benefit that it is also an ultrafast technique, and so we also used it to time-resolve the injection of electrons from the dyes into the TiO_2 . For a model compound that we started with, we discovered that the molecule adopted two different conformations on the TiO_2 surface and that one of those conformations had an electron injection time that was at least 10 times faster than the other. To my knowledge, no one had so definitively shown multiple conformations and certainly no one had resolved different injection rates on the same sample. The general thinking is that fast electron injection leads to higher efficiency. Thus, if one were trying to optimize a solar cell, one would presumably try to maximize the number of molecules that bind in the preferential conformation.

Your pulse-shaping approach has been extended to 2D visible spectroscopy. What is the status of that work?

Zanni: Soon after collecting our first 2D IR spectrum using a mid-IR pulse shaper we realized that a similar approach could be used to collect 2D visible spectra as well. My research group did not own a visible pulse shaper, so I called a good

friend of mine, Niels Damrauer at the University of Colorado. Niels is an expert in pulse shaping and so within a couple of months he had written the computer code to generate the visible pulse sequences and we got our spectra. As I stated above, visible pulse shaping has been around for 20 years so there are many researchers worldwide with the equipment already in their labs to perform experiments like these. There are quite a few groups that have now mimicked our work in this regard and are looking at very interesting materials and biological systems.

What are the next steps in your work on this method?

Zanni: We have just performed experiments that I think are a new technological and intellectual milestone in 2D visible spectroscopy. I think that it will enable many new insights into polymer and molecular photovoltaics. But it isn't published yet, so you'll just have to wait a few months.

References

- (1) P. Hamm, M.H. Lim, and R.H. Hochstrasser, *J. Phys. Chem. B* **102**(31), 6123–6138, DOI: 10.1021/jp9813286 (1998).
- (2) S.-H. Shim, R. Gupta, Y.L. Ling, et al. *Proc. Natl. Acad. Sci. U. S. A.* **106**(16), 6614–6619, DOI: 10.1073/pnas.0805957106 (2009).
- (3) C.T. Middleton, P. Marek, P. Cao, et al., *Nat. Chem.* **4**(5), 355–360, DOI: 10.1038/NCHEM.1293 (2012).



Martin Zanni, PhD, is the Meloche-Bascom Professor of chemistry at the University of Wisconsin-Madison. Direct correspondence to: zanni@chem.wisc.edu

For more information on this topic, please visit our homepage at: www.spectroscopyonline.com

HUMAN HEALTH

ENVIRONMENTAL HEALTH

FT-IR IMAGING THAT'S CLEARLY MEASURABLY AMAZING



Spotlight™ 400 FT-IR Imaging System

There's clarity, and then there's *this* kind of clarity: The Spotlight 400 FT-IR imaging system delivers uncompromising data quality for a more complete, highly detailed picture of the chemical composition of all your samples – regardless of shape and size. And that means faster time to results, quicker product development and more streamlined manufacturing processes – and a better understanding of a wide range of materials, from food packaging to biological tissues. Plus, its ease-of-use features deliver clarity you don't have to be an expert to see and use. The choice for FT-IR imaging in a wide range of industries?

It's clear: Spotlight 400 FT-IR.

www.perkinelmer.com/SpotlightsRange


PerkinElmer[®]
For the Better

Quantification of the Soluble Solids Content of Intact Apples by Vis–NIR Transmittance Spectroscopy and the LS-SVM Method

The feasibility of quantifying the soluble solids content of intact apples was investigated by visible and near infrared (vis–NIR) transmittance spectroscopy combined with the least squares support vector machines (LS-SVM) method. The spectra were pretreated by Savitzky-Golay smoothing, first and second derivatives, standard normal variate transformation, and multiplicative scatter correction. The regression models were developed by LS-SVM and partial least squares (PLS). The accuracy of the LS-SVM and PLS models was compared.

Yande Liu and Yanrui Zhou

Apples are a very popular fruit in people's daily lives because of their delicious taste and nutritional value. Soluble solids content (SSC) is one of the most important evaluation criteria affecting the consumers' appreciation for selection. However, the traditional measurement methods have many disadvantages, such as long analysis time, high costs, and complications.

Visible–near infrared (vis–NIR) spectroscopy is a rapid, reliable, and nondestructive approach for the measurement of SSC in several fruits. Many researchers have reported using nondestructive techniques to assess the SSC value of fruits. In 2004, Chauchard and colleagues (1) showed that the least squares support vector machines (LS-SVM) method was more accurate in prediction than partial least square (PLS) and multiple linear regression (MLR) for predicting the total acidity in fresh grapes. In 2006, Zude and colleagues (2) applied acoustic impulse resonance frequency sensors and miniaturized vis–NIR spectrometers to predict fruit flesh firmness and SSC when the fruit was still on the tree as well as its shelf life. As a result, SSC prediction of freshly harvested apples had a standard error of cross validation (SECV) of $1.29\text{ }^{\circ}\text{Bx}$. In 2009, Fan and colleagues (3) investigated fruit orientation in the examination of SSC in red Fuji apples by vis–NIR transmittance spectroscopy and concluded that the best fruit orientation was when the stem–calyx axis was vertical and the fruit surface was illuminated from the upper side. Also in 2009, Paz and colleagues (4) performed a comparative study which was made

of the performance of different spectrophotometers as part of some research into the potential of NIR reflectance spectroscopy as a nondestructive method for predicting soluble solids content. Many publications have proven that multivariate calibration methods in NIR spectroscopy for estimating varieties of fruit properties are a good alternative (5,6). Although linear models such as multiple linear regression (MLR), principal component regression (PCR), and PLS are widely used in the prediction of fruit quality, nonlinear calibration methods often have better performance, especially in improving the robustness of NIR spectroscopy. Support vector machines (SVM) is a powerful methodology for solving problems in nonlinear classification, function estimation, and density estimation. LS-SVM is an improved method of standard SVM put forward by Suykens and Vande in 1999 and Suykens and colleagues in 2002. It transformed the quadratic programming problem of a standard SVM demand solution to a linear problem by using the least square value function and equality constraints and increased the training speed and restraining precision. Some researchers have applied LS-SVM to regression models. Kovalenko and colleagues (7) determined amino acid composition of soybeans and concluded that the performance of LS-SVM was better than that of artificial neural networks (ANN). Sun and colleagues reported that LS-SVM models were better than PLS models with correlation coefficient (R) and root mean square error of prediction (RMSEP) of (0.88, $0.80\text{ }^{\circ}\text{Bx}$) and (0.82, $1.01\text{ }^{\circ}\text{Bx}$) for portable and on-line measurement mode,

USP <735> INTRODUCES A NEW CHAPTER IN USP <232>

Meet new regulations for elemental impurities with XRF

Getting ready to meet the new regulations for Elemental impurities set forth in USP<232>? Be sure to look at the smart alternative to ICP: X-ray Fluorescence (XRF). USP <735> introduces XRF as an accepted technique for Elemental Impurities <232> and <233> analysis in the pharmaceutical industry.



Key Advantages of XRF:

Easy and fast sample preparation - analyze solids, powders or liquids as is, no need to dissolve or dilute

Faster sample throughput time - all elements in USP<232>

Reduced operational costs - no chemicals or hazardous waste stream

Lower TCO than other instruments capable of USP <232> compliance

Robust instrumentation with long lasting (years) calibration

Non-destructive - sample can fully recovered and used for further testing

According to USP
<232> ELEMENTAL IMPURITIES - LIMITS
<2232> ELEMENTAL CONTAMINANTS IN DIETARY SUPPLEMENTS
<735> X-RAY FLUORESCENCE SPECTROMETRY



PANalytical's Epsilon 5



PANalytical Inc.
117 Flanders Road
Westborough, MA 01581, USA
T +1 508 647 1100
F +1 508 647 1115
Toll Free: +1 800 279 7297
ask@panalytical.com
www.panalytical.com

The Analytical X-ray Company



PANalytical

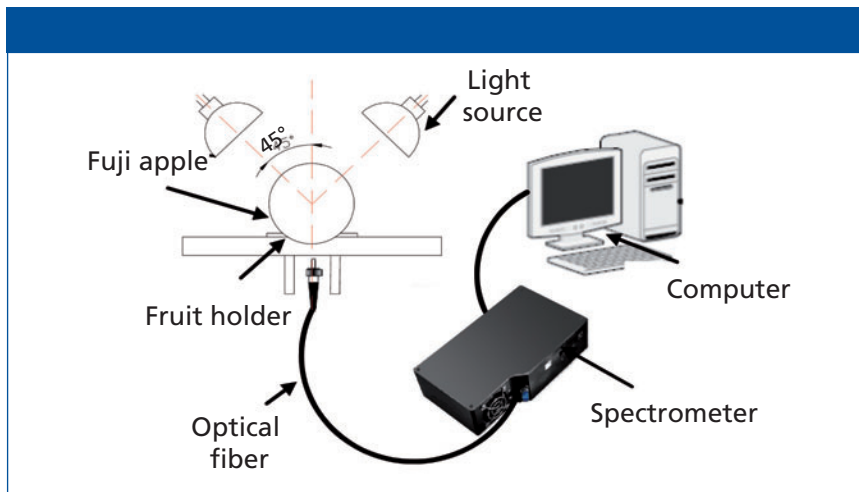


Figure 1: Schematic diagram of NIR acquisition device.

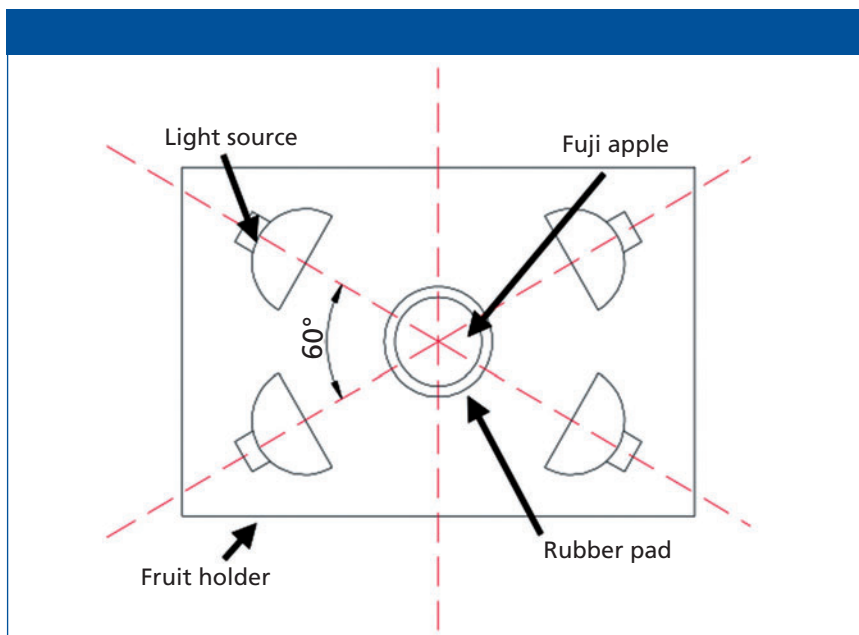


Figure 2: Top view of light source and apple.

respectively (8). Liu and colleagues (9) developed an NIR spectrometry regression model by LS-SVM, and the results showed that portable NIR combined with LS-SVM was a feasible method to predict Brix values of intact pears non-destructively. Also, Liu and colleagues (10) investigated the performance of NIR spectrometers with LS-SVM in determining acetic, tartaric, and formic acids, and the pH of fruit vinegars. The results indicated that NIR spectroscopy ($7800\text{--}4000\text{ cm}^{-1}$) combined with LS-SVM could be utilized as a precision method for the determination of organic acids and pH of fruit vinegars. In addition, Liu and colleagues (11) applied principal component analysis (PCA) combined with partial least-squares discriminant (DPLS) and LS-SVM to realize the rapid identification of different varieties of pears. Both of those two models had preferable results, that the rate of identification is 100%. Nie and colleagues (12) investigated the performance of vis-NIR spectroscopy as a rapid and nondestructive technique to determine the boiling time of yardlong beans. Pissard and colleagues (13) determined the vitamin C, polyphenol, and sugar contents in apples by NIR spectroscopy combined with the LS-SVM method.

The objectives of this study were to investigate the feasibility of using vis-NIR spectroscopy combined with the LS-SVM method to predict the SSC of intact apples nondestructively and to compare the accuracy of the LS-SVM and PLS models.

Materials and Methods

Sample Preparation

A total of 160 Fuji apples were obtained from a local fruit supermarket near Nanchang, Jiangxi province in China. The apple samples were stored at $20\text{ }^{\circ}\text{C}$ constant temperature and 60% relative humidity for 24 h before vis-NIR spectra measurement. After that, three separate signs were made on the equator of each apple with the locations 120° apart, avoiding any obvious surface defects (such as bruises or scars).

Spectral Data Acquisition

NIR diffuse reflectance spectra in the $200\text{--}1100\text{ nm}$ region were obtained with

Table I: Characteristics of calibration and prediction set

Data set	N	Max	Min	Mean	SD	CV (%)
Calibration set	120	16.17	8.8	13.00	1.20	9.21
Prediction set	40	16.15	10.5	13.44	1.66	12.23

N = number of samples; SD = standard deviation; CV = coefficient of variation

Table II: Statistical results of PLS models with different pretreatment methods

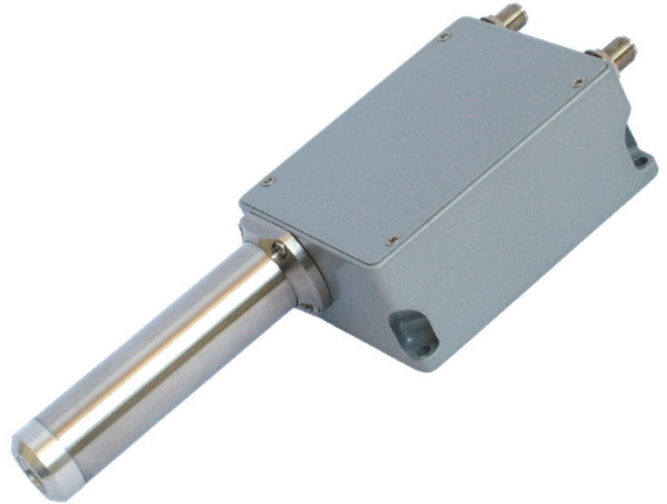
Pretreatment Methods	LVs	r_c	SEC	r_p	SEP
Origin	12	0.94	0.40	0.90	0.53
1Der + MSC + smoothing	11	0.95	0.39	0.91	0.51
1Der + SNV + smoothing	11	0.94	0.40	0.90	0.52
2Der + MSC + smoothing	10	0.92	0.48	0.82	0.69
2Der + SNV + smoothing	11	0.93	0.44	0.84	0.65

r_c = the correlation coefficient of the calibration set; r_p = the correlation coefficient of the prediction set



XRF200i - compact silicon drift detectors (SDD) designed for OEM bench-top XRF applications.

SGX Sensortech have a distinguished heritage in the manufacture of Silicon Drift (SDD) and Si(Li) detectors. Previously known as e2v scientific and Gresham Scientific, SGX specialises in producing detectors from standard designs through customised assemblies to complex multi-element detectors. XRF200i are compact silicon drift detectors (SDD) designed for OEM bench-top XRF applications. Sensors are hermetically sealed and cooled by thermo-electric devices. The detectors incorporate transistor reset preamplifiers and temperature control circuits which maintains the guaranteed energy resolution over a +10°C to +40°C temperature range. Excellent peak to background performance is achieved over a wide x-ray acceptance angle range by means of 'on-chip' internal collimation.



Features

- Sensor collimated areas from 7mm² to 80mm²
- Thickness 0.45mm
- Multi-Z on chip collimation
- UTW (AP3.3) or Be windows available
- Temperature controller
- Low voltage and bias power supply
- Vacuum compatible

Performance

- Typical resolution 128eV
- Resolution specification 133eV
- Peak to background > 10000:1

Physical

- Case size; 77 x 58 x 30 mm excluding tube and connectors
- 4 fixing holes for heat sinking
- Tube length 300mm max, diameter 18.5 mm
- Weight: 570g

Available with active areas from 10mm² to 100mm²

Active Area (mm ²)	10	25	30	40	60	100
Collimated area (mm ²)	7	15	20	30	50	80
Resolution (eV)	130	130	130	130	130	130

To fully exploit the high rate capability, the XRF200i may be paired with the DX200 Digital Pulse Processor. DX200 parameters are USB controlled, with spectrum transfer available via USB or real time event by event data via 20 way parallel port. The DX200 utilizes a fast 16bit 40Mhz ADC and has fast recognition circuits for excellent pile-up rejection. It is bundled with Data transfer software.



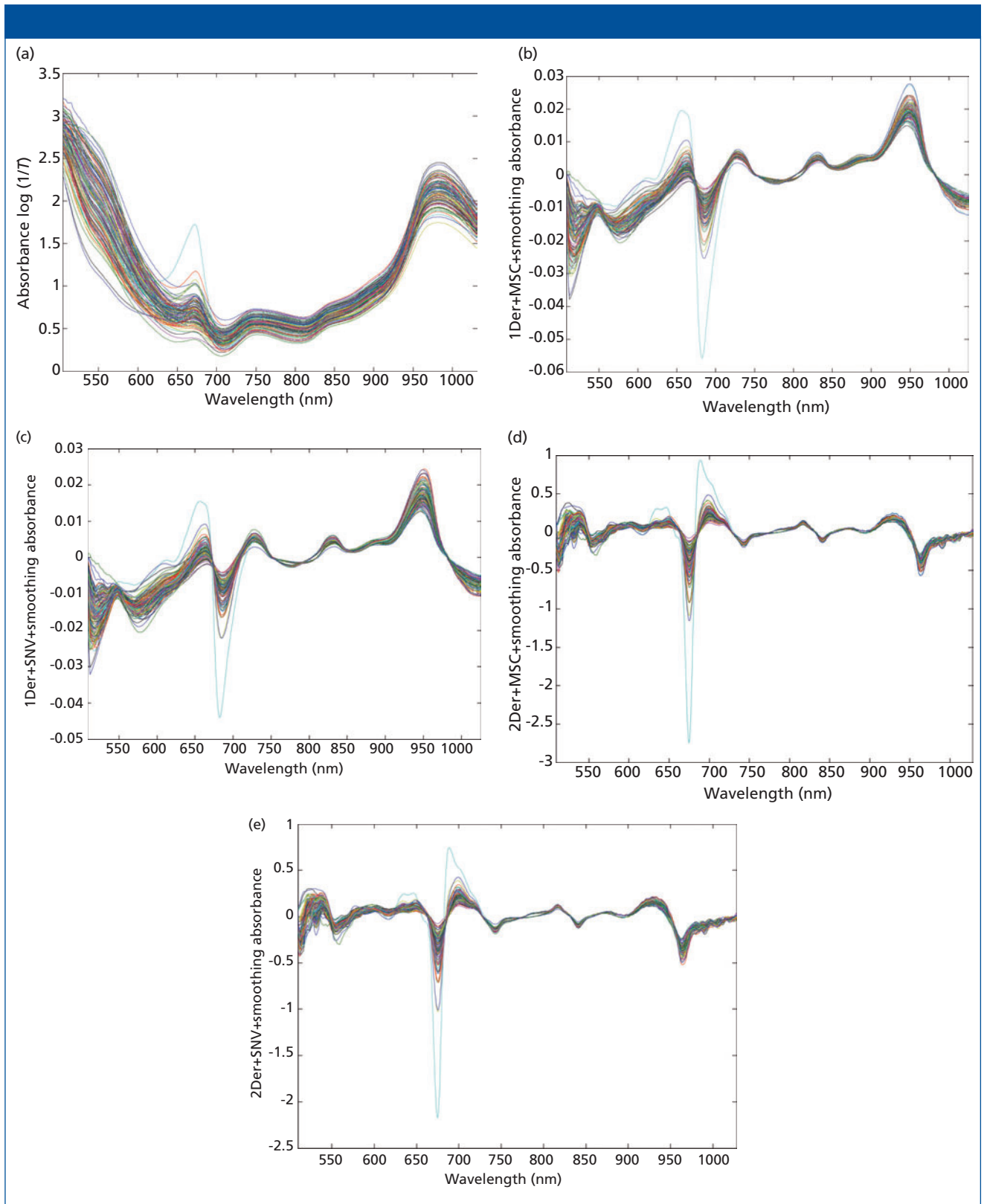


Figure 3: (a) The original absorbance spectra and preprocessed spectra by (b) 1Der + MSC + smoothing, (c) 1Der + SNV + smoothing, (d) 2Der + MSC + smoothing, and (e) 2Der + SNV + smoothing.

NIR spectrometry equipment that consisted of four light sources that could be used both in the visible and near infra-

red region, 350–1650 nm (type reference: 41850SP, 12 V, 50 W, halogen, Osram lamps), a spectrometer, a fiber-optics

probe (74-UV, Ocean Optics), an optical fiber, a fruit holder or light collection fixture, a computer system with Spectra-

Suite software (Ocean Optics), and other accessories. The transmission mode was applied for this experiment. The four light sources were placed at a height of about 200 mm above the sample. The fiber spectrometer used in this experiment was a model QE65000 system from Ocean Optics. This spectrometer was equipped with a 1044 horizontal \times 64 vertical element linear silicon charge-coupled device (CCD) detector with a wavelength range of 200–1100 nm. The probe of the spectrometer was placed under and close to the sample. The arrangement of the equipment is shown in Figures 1 and 2. As for the spectrometer parameter setting, integration time was 100 ms, smoothness was 15, and the average number was 1. Before the spectrum collection of individual apple samples, the dark current and the reference should be measured. In this process, air was used as the reference. The spectra of all individual fruit were measured at three positions that were signed around the equator, approximately 120° apart, and perpendicular to the stem–calyx axis. The spectra of the samples were calculated as an average of the three measurements.

SSC Reference Measurement

To build the calibration and the validation models, the real quality parameters of individual fruit should be assessed. The SSC values of the apples were determined using a conventional destructive testing method. The SSC values of apples were determined immediately after vis-NIR spectroscopy measurements using a digital refractometer (PR-101 α , ATGO). The measurement accuracy is ± 0.1 °Bx, and the measurement range is 0–45.0 °Bx with automatic temperature compensation.

Regression Model

PLS Model

Because PLS is already widely used in mathematical algorithms for multivariate linear regression, the theory of these methods will not be presented explicitly herein. The principle behind the PLS algorithm is to correlate the spectrum x_i^T , and reference value y_p , of all the samples in X and compress it in a set of new independent latent variables. The predic-

tions \hat{y} are computed by the following equation:

$$\hat{y} = X \hat{\beta} + \hat{b}_0 \quad [1]$$

Where $\hat{\beta}$ is a ($p \times 1$) vector of regression coefficients; and \hat{b}_0 is the model offset (1).

LS-SVM Model

The SVM method has been proven to be a useful approach for solving problems in nonlinear classification, function estimation, and density estimation. SVM

is based on statistical learning theory related to the principle of structural risk minimization.

LS-SVM is an optimized algorithm based on the standard support vector machine proposed by Suykens (14). LS-SVM has a good theoretical foundation in the statistical learning method and the capability of dealing with linear and nonlinear multivariate calibration (15,16). The details of the LS-SVM algorithm can be found in the literature (14).

In LS-SVM function estimation,

BWTEK INC.
SPECTROMETERS | LASERS | TOTAL SOLUTIONS
Your Spectroscopy Partner

Smart
... & Packed with Power!

Exemplar Plus
BWTEK Your Spectroscopy Partner

Introducing the all-new Exemplar Plus

The Exemplar Plus provides high sensitivity, high resolution, high dynamic range and low straylight combined with our cutting edge smart spectrometer technology.

Smart, fast and plays wells with others. See the entire line-up of the synchronizable Exemplar spectrometer series.

Ideal for:

- Reaction Monitoring
- Fluorescence
- Raman
- LIBS

Call 1-855-MY-BWTEK today & keep your lab on the cutting edge!
www.bwtek.com



Retsch®
Solutions in Milling & Sieving

Sample Preparation
For Analytical Excellence!

If you are looking for a complete line of products for sample preparation, look no further than RETSCH.

PURE SCIENCE — NO FICTION

- Mills and grinders for all sample types
- Fast, reproducible results every time
- Wide variety of grinding tools
- German engineered for many years of reliable service
- Easy to use, clean and maintain

ZERO GRAVITY

Win an extraordinary adventure or total prizes worth **10,000 €**

www.retsch.com/win

Legal action excluded

1-866-4-RETSCH

WWW.RETSCH.COM part of **VERDER scientific**

Table III: Performance comparison for SSC prediction models developed by PLS and LS-SVM

Type of model	r_c	SEC	r_p	SEP
PLS	0.95	0.39	0.96	0.45
LS-SVM	0.98	0.24	0.98	0.29

r_c = calibration set correlation coefficient; r_p = prediction set correlation coefficient

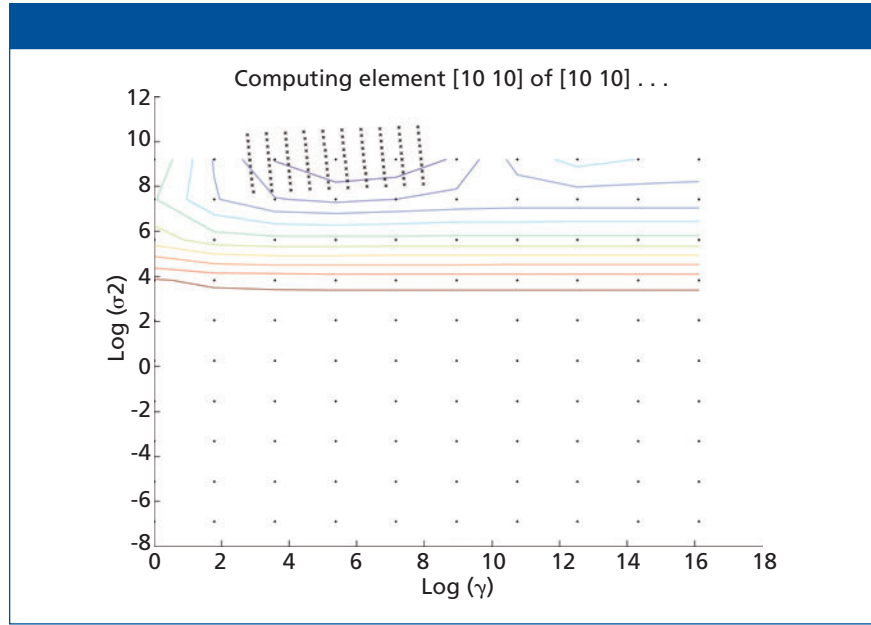


Figure 4: Contour plot of the optimization the parameters γ and σ^2 .

the standard framework is based on a primal-dual formulation (17). Suppose the training samples are $\{x_i, y_i\}$ ($i = 1 \dots N$) in which $x_i \in R^n$ is an input parameter and $y_i \in R$ is an output parameter of sample number. In SVM, the data is nonlinearly mapped to form the input space to a high dimensional feature space using $\varphi(x)$. The estimated function is introduced as

$$y(x) = \omega^T \phi(x) + b + e_i \quad [2]$$

where ω is the adjustable weight and b is the bias term. The following optimization problem is formulated:

$$\min_{\omega, b, e} J(\omega, e) = \frac{1}{2} \omega^T \omega \quad [3]$$

+ $\gamma \frac{1}{2} \sum_{i=1}^N e_i^2$

subject to $y_i[\omega^T \varphi(x_i) + b] = 1 - e_i, i = 1 \dots N$ where γ is the regularization parameter which balances the model's complexity and the training errors, and e_i represents the random errors.

This optimization problem can be

solved in a dual space. To solve the problem, the following Lagrangian is defined:

$$L(\omega, b, e, \alpha) = J(\omega, e) - \sum_{i=1}^N \alpha_i \quad [4]$$

$$\alpha_i \{ \omega^T \phi(X_i) + b + e_i - y_i \}$$

where α_i are the Langrange multipliers called *support value*. The solution of the above equation can be obtained by partially differentiating with respect to ω, b, e_p and α_i

$$\begin{cases} \frac{\partial L}{\partial \omega} = 0 \rightarrow \omega = \sum_{i=1}^N \alpha_i \varphi(X_i) \\ \frac{\partial L}{\partial b} = 0 \rightarrow \sum_{i=1}^N \alpha_i = 0 \\ \frac{\partial L}{\partial e_i} = 0 \rightarrow \alpha_i = \gamma e_i, \quad i = 1, \dots, N \\ \frac{\partial L}{\partial \alpha_i} = 0 \rightarrow \omega^T \varphi(x_i) + b + e_i - y_i = 0, \quad i = 1, \dots, N \end{cases} \quad [5]$$

By the elimination of ω and e_p , the following linear system is obtained:

$$\begin{bmatrix} 0 & \mathbf{1}^T \\ \mathbf{y} & \Omega + \gamma^{-1} \mathbf{I} \end{bmatrix} \begin{bmatrix} b \\ \beta \end{bmatrix} = \begin{bmatrix} 0 \\ \mathbf{y} \end{bmatrix} \quad [6]$$

where $\gamma = [\gamma_1, \dots, \gamma_n]^T$; $\beta = [\beta_1, \dots, \beta_n]^T$; $\Omega = \approx (x_i)^T \zeta(x_n)$.

The LS-SVM model can be defined as follows (14):

$$y(x) = \sum_{i=1}^n \alpha_i K(x, x_i) + b \quad [7]$$

Where $K(x, x_i)$ is a kernel function.

The robustness of LS-SVM models is largely determined by the crucial elements of optimal input feature subset, proper kernel function, and optimum kernel parameters. To improve the training speed and reduce the training error, available latent variables (LVs) that were applied as inputs of LS-SVM models were necessary.

The PLS method to determine LVs was used in the LV-SVM model to ensure that all variability was considered by the analysis. Commonly used kernel functions are linear_kernel, polynomial_kernel, and RBF_kernel. However, there is no systematic methodology for the selection of a kernel function. The optimal parameters of each kernel function are found from an intensive grid search and leave-one-out cross-validation and selected when resulting in smaller root mean square error of cross-validation (RMSECV). Grid search is a two-dimensional minimization procedure based on an exhaustive search in a limited range. In each iteration, one leaves one point, and fits a model on the other data points. The performance of the model is estimated based on the point left out. This procedure is repeated for each data point. The LS-SVM model was carried out using MATLAB (Mathworks) and free LS-SVM software for MATLAB (LS-SVM v1.5, Suykens, Leuven, Belgium).

The standard error of calibration (SEC), the standard error of prediction (SEP), and the correlation coefficient (r) were used to measure the model's performance. The SEC, SEP, and r are calculated as follows:

$$SEC = \sqrt{\frac{1}{n_c} \sum_{i=1}^{n_c} (y_i - \hat{y}_i)^2} \quad [8]$$

$$SEP = \sqrt{\frac{1}{n_p} \sum_{i=1}^{n_p} (y_i - \hat{y}_i)^2} \quad [9]$$

$$r = \sqrt{1 - \frac{\sum_{i=1}^n (y_i - \hat{y}_i)^2}{\sum_{i=1}^n (y_i - \bar{y})^2}} \quad [10]$$

Where γ_i and $\hat{\gamma}_i$ are the measurement and prediction value of the samples, $\bar{\gamma}$ is the mean value of γ_i , n_c and n_p is the number of apples in the calibration set and the prediction set. The value n is equal to n_c or n_p .

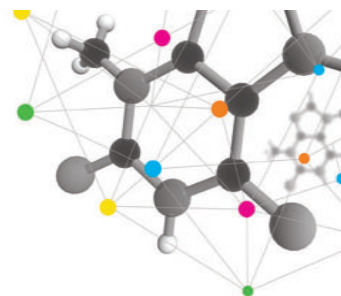
Results and Discussion

Calibration and Validation Sets

All samples were randomly divided into calibration sets of 120 samples and prediction sets of 40 samples (18). No single sample was used in calibra-

tion and prediction sets at the same time. To ensure the adaptability of the calibration models, the samples with high and low SSC values were put in the calibration set, and the other sample selections inside each group were performed randomly. To compare the performance of different calibration models, the samples in the calibration and prediction sets were kept unchanged for all calibration models. The calibration and prediction set data are presented in Table I.

ChemLogix™



THE LOGICAL CHOICE FOR RAPID CHEMICAL ANALYSIS OF SOLID MATERIALS

Introducing the ChemLogix™ Family of Chemical Analysis Instruments, Including the ChemReveal™ LIBS Desktop Analyzer

The ChemLogix™ family of instruments simplifies complex chemical analysis.

Its line of ChemReveal™ laboratory-based analyzers utilizes laser-induced breakdown spectroscopy (LIBS) to provide rapid and reliable identification of materials and chemical composition of solids.

Equipped with advanced ChemLytics™ software and backed by TSI's global sales and support, ChemLogix instruments truly are the smarter - and more logical - choice for chemical analysis.

Understand more, visit tsi.com/ChemReveal



UNDERSTANDING, ACCELERATED

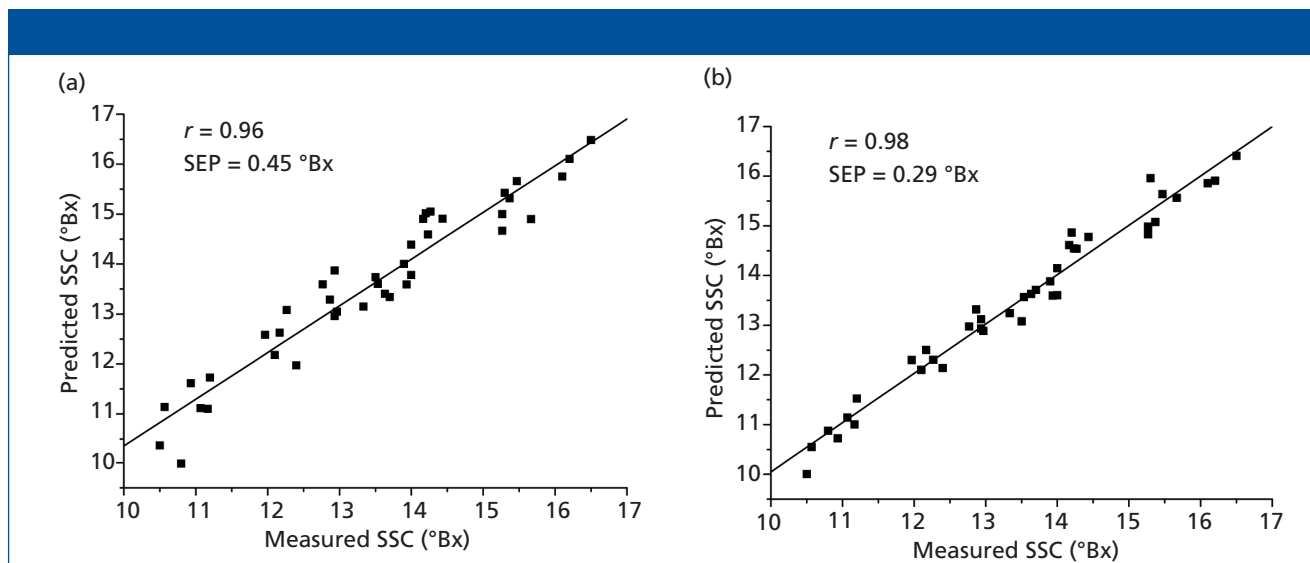


Figure 5: The prediction plots of PLS and the LS-SVM model: (a) Prediction plots: measured SSC vs. predicted SSC for PLS model; (b) prediction plots: measured SSC versus predicted SSC for the LS-SVM model.

Data Preprocessing

Three transmittance spectra of each sample were averaged into one spectrum, and then the averaged spectrum was transformed into an absorbance spectrum using the $\log(1/T)$ relationship. Because of obvious scattering, noise could be observed at the beginning and the end of the spectral data. Thus, the first 300 nm and the last 69 nm data were eliminated to improve the measurement accuracy and speed, so the spectral analysis was based on 505–1031 nm wavelengths (3). To reduce spectral

noise and enhance the useful information, several spectral pretreatment methods were applied. These methods included Savitzky-Golay smoothing (smoothing) with a window width of 5 points and 0 order polynomial to eliminate the random noise, Savitzky-Golay first derivative (1Der) with a window width of 3 points and second order polynomial, and Savitzky-Golay second derivative (2Der) with a window width of 5 points and second order polynomial to remove baseline shifts and make superimposed peaks more obvious, standard

normal variate transformation (SNV) to remove slope variation and correct scatter effects in spectra, and multiplicative scatter correction (MSC) to remove these effects by linearizing each spectra to the average spectra, respectively (19). In this paper, four combinations of pretreatment methods were used to preprocess the sample spectra: 1Der + MSC + smoothing; 1Der + SNV + smoothing; 2Der + MSC + smoothing; and 2Der + SNV + smoothing. All of these pretreatment methods were carried out using Unscrambler V8.0 software (CAMO

It's much better without a gap.


Cells

Micro Volume Analysis

▶ UV/Vis Calibration Standards

Fiber Optical Systems


Micro Flow Channels



Now available:

The new calibration manual offering many useful tips.

hellma-analytics.com/tips




With the use of UV/Vis calibration standards from the accredited calibration laboratory of Hellma Analytics, you ensure the complete traceability of your measurement results. Regular calibration of your spectrophotometer provides a continuously high measuring quality, process reliability and conformity to DIN ISO, GLP or Pharmacopoeia regulations. Call 516-939-0888 or visit www.hellmausa.com

The Hellma Analytics calibration laboratory

Accredited acc.

DIN EN ISO 17025



High Precision in Spectro-Optics

AS). The original absorbance spectra and pretreatment spectra of the samples are shown in Figure 3.

All of the combinations of different pretreatment methods had an effect on reducing the number of LVs for PLS models; the results are presented in Table II. In contrast, the combination of 1Der + MSC + smoothing had a better performance than others ($r = 0.91$, $SEP = 0.51$). Therefore, the combination of 1Der + MSC + smoothing was applied in this work.

LS-SVM Model

Selection of Inputs of LS-SVM

To improve the computational speed and training accuracy of the vis-NIR model, suitable LVs were selected as inputs for the LS-SVM model. The LVs that were selected could explain most of the spectral variances and represent the main information of the original spectra to the measured chemicals. We applied the PLS method to obtain the optimal input feature subset for LS-SVM. By means of PLS, the first 11 important

LVs were regarded as the inputs of the LS-SVM model according to the smallest prediction residual error sum of squares (PRESS). Therefore, the optimal number of LVs for the LS-SVM model could be achieved by the PLS method and the computational time of the LS-SVM model could be reduced at the same time.

Tuning the Parameters of LS-SVM

There are three kinds of commonly used kernel functions named linear_kernel, polynomial_kernel, and RBF_kernel. Compared to first two kernel functions, the RBF_kernel has many advantages. For example, the nonlinear relationships between the spectra and target attributes can be handled and the computational complexity of the training procedure can also be reduced with good performance under general smoothness assumptions. The RBF_kernel was introduced in detail. The gam (γ) and sig2 (σ^2) are two important parameters for the RBF_kernel function, which were similar to the process used to select the number of LVs

for the PLS models, but in this case it is a two-dimensional problem. Parameters are selected by a grid-search technique based on leave-one-out cross validation, which was used to avoid over-fitting. The ranges of γ and σ^2 within (10^{-2} – 10^6) were set based on experience and previous studies (20–22). For each combination of γ and σ^2 parameters, the RMSECV was calculated and the optimum parameters were selected to produce smaller RMSECV. The contour plot of the optimization the parameters γ and σ^2 for the prediction of SSC is shown in Figure 4. The first step in the grid search was for a crude search with a larger step size presented in the form of “.”, and the number of the grids “.” was 10×10 . The optimal search area was determined by an error contour line. The second step for the specified search with a smaller step size presented in the form of “×”, and the number of grids “×” was 10×10 . The optimal search area is determined based on the first step. The optimal combination of (γ , σ^2) was achieved with $\gamma = 2452.07$ and $\sigma^2 = 42354.90$ for SSC.

FACSS
40TH
ANNIVERSARY

THE GREAT SCIENTIFIC EXCHANGE
SciX 2013
presented by FACSS



SciXConference.org
FACSS.org

Milwaukee, WI • Sept. 29 - Oct. 4, 2013 • Hyatt Regency Milwaukee and Delta Center

The Premier Conference in Analytical Spectroscopy

Featuring sessions in Biomedical Analysis, Security and Forensics, Surface Science, Pharmaceuticals, Nanotechnology, Chemometrics, Laser-Induced Breakdown Spectroscopy, Process Analytical, Raman, Infrared, NIR and more.

Leaders in Spectroscopy Featured in Major Awards Sessions

Strock Award – Rick Russo

Mann Award – Volker Deckert

Meggers Award – Paul Pudney

Anachem Award – Norm Dovichi

Craver Award – Rohit Bhargava

ACS Award – Charles Wilkins



NATIONAL MEETING OF: Society for Applied Spectroscopy (SAS) and
The North American Society for Laser-Induced Breakdown Spectroscopy



Introducing the SPECTROSCOPY APP for your iPhone or iPad



Designed for both the iPhone and iPad, *Spectroscopy's* new app may be found on iTunes, under the Business category, and downloaded for free. Exploring the latest news and trends for spectroscopists has never been easier.

Download it for free today at
[http://www.spectroscopyonline.com/
SpectroscopyApp](http://www.spectroscopyonline.com/SpectroscopyApp)

Comparison of PLS and LS-SVM Models

The prediction set with 40 samples was predicted by the PLS model built with 11 LVs and LS-SVM model with the optimal parameters: $\gamma = 2452.07$, $\sigma^2 = 42354.90$. Performance comparison between PLS and LS-SVM is listed in Table III. From Table III, it can be observed that the prediction performance of LS-SVM was better than that of PLS, with higher r of 0.98 and lower SEP of 0.29 for SSC. The prediction plots of PLS and LS-SVM model are shown in Figure 5. Based on the results, it was concluded that vis-NIR transmittance spectroscopy combined with LS-SVM was a reliable and accurate method for the determination of SSC of apples. For SSC determination, the performance of this LS-SVM model was better than previous similar research. Bessho and colleagues (23) applied a new portable nondestructive quality meter with NIR spectroscopy to measure soluble solids ($r = 0.8$, $SEP = 0.5$ °Bx) of apple. Fan and colleagues (3) predicted firmness ($r^2 = 0.8532$, $SEP = 0.3838$) and SSC ($r^2 = 0.8136$, $SEP = 0.5344$). Huang and colleagues (24) predicted total soluble solid contents (TSS) and pH in mulberry fruit, and coefficients of determination for prediction (r_{pre}^2) values were 0.70 for TSS and 0.90 for pH. Chen and colleagues (25) determined the antioxidant activity (AA) ($R_p = 0.9691$, $RMSEP = 0.02161$) in green tea, using NIR spectroscopy and support vector machine regression (SVMR).

Conclusions

In this paper, the feasibility of quantification SSC of intact apples was investigated by vis-NIR transmittance spectroscopy combined with the LS-SVM method. The PLS models were developed and compared using different combinations of spectral pretreatment methods including 1Der + MSC + smoothing, 1Der + SNV + smoothing, 2Der + MSC + smoothing, and 2Der + SNV + smoothing. The best prediction performance was achieved by 1Der + MSC + smoothing. Moreover, to optimize the LS-SVM models, optimal LVs were selected by regression coefficients. Meanwhile, the accuracy of the LS-SVM models and PLS models was compared. The results indicated that the combination of LS-SVM, 1Der + MSC + smoothing, and the optimal latent variables from PLS ($r = 0.98$, $SEP = 0.29$) outperformed the other methods. Finally, it can be concluded that vis-NIR spectroscopy combined with LS-SVM could be a promising method for the regression analysis to quantify the SSC value of apples.

Acknowledgment

Financial support was provided by the National High Technology Research and Development Program of China (863Program) (No. 2012AA101906), the Ministry of science and technology of agricultural achievements into capital projects (No. 2011G132C500008), Ganpo excellence project 555 Talent Plan of Jiangxi Province (2011-64), Center of Photoelectric Detection Technology Engineering of Jiangxi Province (2012-155).

References

- (1) F. Chauchard, R. Cogdill, S. Roussel, J.M. Roger, and V. Bellon-Maurel, *Chemom. Intell. Lab. Syst.* **71**, 141–150 (2004).

- (2) M. Zude, B. Herold, J. Roger, V. Bellon-Maurel, and S. Landahl, *J. Food Eng.* **77**, 254–260 (2006).
- (3) G.Q. Fan, J.W. Zha, R. Du, and L. Gao, *J. Food Eng.* **93**, 416–420 (2009).
- (4) P. Paz, M. Sánchez, D. Pérez-Marín, J.E. Guerrero, and A. Garrido-Varo, *Computers and Electronics in Agriculture* **69**, 24–32 (2009).
- (5) S. Saranwong, J. Sornsriwichai, and S. Kawano, *Near Infrared Spectroscopy*. **11**, 175–181 (2003).
- (6) F. Liu, Y. He, and W. Li, *Anal. Chim. Acta* **615**, 10–17 (2008).
- (7) L.V. Kovalenko, G.R. Rippke, and C.R. Hurburgh, *Journal of the American Oil Chemists' Society* **83**, 421–427 (2006).
- (8) X.D. Sun, H.L. Zhang, Y.Y. Pan, and Y.D. Liu, *Photonics and Optoelectronics Meetings (POEM)* **7514**, 1–7 (2009).
- (9) Y.D. Liu, R.J. Gao, X.D. Sun, A.G. OuYang, and Y. Y. Pan, presented at the Sixth International Conference on Natural Computation, Yantai, China, 909–913 (2010).
- (10) F. Liu, Y. He, L. Wang, and G.M. Sun, *Food Bioprocess Technol.* **4**, 1331–1340 (2011).
- (11) X.M. Liu and H.L. Zhang, *Trans. Chin. Soc. Agric. Mach.* **43**, 160–164 (2012) (in Chinese).
- (12) P.C. Nie, D. Wu, Y. Yang, and Y. He, *J. Food Eng.* **99**, 155–161 (2012).
- (13) A. Pissard, P.J.A. Fernández, V. Baeten, G. Sinaeve, G. Lognay, A. Mouteau, P. Dupont, A. Rondia, and M. Lateur, *J. Sci. Food Agric.* **93**, 238–244 (2013).
- (14) T.V. Gestel, J.A.K. Sunkens, B. Baesens, S. Viaene, G. Dedene, B.D. Moor, and J. Vandewalle, *Machine Learning*, **54**, 5–32 (2004).
- (15) V.N. Vapnik, *The Nature of Statistical Learning Theory* (Springer Press, Germany, 2000), pp. 156–223.
- (16) J.A.K. Suykens and J. Vandewalle, *Neural Processing Letters* **9**, 293–300 (1999).
- (17) M.W. Mustafa, M.H. Sulaiman, H. Shareef, and S.N. Abd. Khalid, *Generation, Transmission and Distribution, IET* **6**, 133–141 (2012).
- (18) F. Liu, Y. He, L. Wang, and G.M. Sun, *Food Bioprocess Technol.* **4**, 1331–1340 (2011).
- (19) A. Savitzky and M.J.E. Golay, *Analytical Chemistry* **36**, 1627–1639 (1964).
- (20) H. Guo, H.P. Liu, and L. Wang, *J. Syst. Simul.* **18**, 2033–2036 (2006).
- (21) Q. Chen, J. Zhao, C.H. Fang, and D. Wang, *Spectrochim. Acta, Part A* **66**, 568–574 (2007).
- (22) A.I. Belousov, S.A. Verzakow, and J. Frese, *J. Chemom.* **16**, 482–489 (2002).
- (23) H. Bessho, K. Kudo, J. Omori, Y. Inomata, M. Wada, T. Masuda, Y. Nakamoto, H. Fujisawa, and Y. Suzuki, *Acta Hort.* **732**, 93–597 (2007).
- (24) L.X. Huang, D. Wu, H.F. Jin, J.K. Zhang, Y. He, and C.F. Lou, *Biosystem Engineering*, **10**, 377–384 (2011).
- (25) Q.S. Chen, Z.M. Guo, J.W. Zhao, and Q. Ouyang, *J. Pharm. Biomed. Anal.* **60**, 92–97 (2012).

Yande Liu is a professor at the Institute of Optics-Mechanics-Electronics Technology and Application (OMETA), in the School of Mechatronics Engineering at East China Jiaotong University in Nanchang, Jiangxi, China.

Yanrui Zhou is a graduate student at the Institute of Optics-Mechanics-Electronics Technology and Application (OMETA), in the School of Mechatronics Engineering at East China Jiaotong University. Direct correspondence to: jluiyd@163.com ■

For more information on this topic, please visit our homepage at: www.spectroscopyonline.com



SPECTROMETERS | LASERS | TOTAL SOLUTIONS

Your Spectroscopy Partner

Innovative

Enhanced & Revolutionary: i-Raman Plus



Now with the most advanced technology

- Deep TE Cooling for up to 30 Minutes of Integration Time
- Highly Sensitive Back-thinned CCD Detector
- Patented CleanLaze® Laser Stabilization
- High Throughput F/2 Spectrograph
- Spectral Resolution as Fine as 3cm⁻¹
- Spectral Range from 65cm⁻¹ to 4000 cm⁻¹
- Fiber Optic Probe for Flexible Sampling
- Sampling Stage, Cuvette Holder, and Chemometric Software Available



HIGHLY SENSITIVE FIBER OPTIC RAMAN SYSTEM

Call now to stay on the cutting edge!

1-855-BW-RAMAN
www.bwtek.com

Denver X-ray Conference: 62nd Annual Conference on Applications of X-ray Analysis

A preview of the upcoming Denver X-ray Conference to be held August 5–9, 2013, in Westminster, Colorado.

Megan Evans, *Spectroscopy* Managing Editor

This year's Denver X-ray Conference will take place August 5–9, at the The Westin hotel in Westminster, Colorado. Here is a brief preview of what to expect from this year's conference, including sessions on training and education, and applications and papers dealing with X-ray analysis techniques and future developments.

Workshops

Workshops will be held Monday and Tuesday, August 5 and August 6, with morning sessions from 9:00 a.m. to 12:00 p.m. and afternoon sessions from 1:30 p.m. to 4:30 p.m. Topics include "Back to Intermediate XRD Analysis," "Basic XRF," "X-ray Optics," "Energy Dispersive XRF," "Hands-On Rietveld Analysis," and "Sample Preparation of XRF" among many others.

Plenary Session and Awards

This year's plenary session topic is "The 100th Anniversary of X-ray Spectroscopy," and will be chaired by G.J. Havrilla of Los Alamos National Laboratory. The session will take place at 9:00 a.m., Wednesday, August 7, and will kick off with opening remarks from the chairman of the conference, W. Tim Elam. After the chairman's comments, the following awards will be presented: the 2013 Barrett Award, which recognizes outstanding contributions to the field of powder diffraction (recipient to be announced); the 2013 Jenkins Award, which honors scientists who exhibit lifetime achievement in the advancement of the use of X-rays in materials analysis, will be presented to Rene Van Grieken of the University of Antwerp; the 2013 Jerome B. Cohen Student Award, which recognizes the outstanding achievements of student research in the field of X-ray analysis (recipient to be announced); and the 2013 Hanawalt Award, which is presented every three years for an important, recent contribution to the field of powder diffraction, will be presented to Robert B. Von Dreele of Argonne National Laboratory.

After the awards are presented, Havrilla will make some remarks and the invited talks will begin. The first talk will be

given by John A. Anzelmo and is titled "WDX: From Roentgen to Moseley to Bragg to Sherman to Jenkins." Next, "The Electronic Age — EDX and Other Modern Techniques to the Present and Beyond," will be presented by Michael Mantler. Finally, Robert B. Von Dreele will present "Hanawalt Award Lecture: Protein Polycrystallography."

In addition to the plenary session, there will be several oral sessions on Wednesday afternoon, Thursday morning and afternoon, and Friday morning. Topics range from high energy X-ray diffraction to micro X-ray fluorescence, stress analysis, trace analysis, and more.

Exhibits and Special Events

Exhibits will be held in the Westminster Ballroom on the lobby level of the Westin Westminster hotel. Exhibit hours are 11:00 a.m. to 5:00 p.m. Monday and Tuesday, 12:00 p.m. to 7:00 p.m. on Wednesday, and 10:00 a.m. to 1:00 p.m. on Thursday. About 30 different companies will be on hand to showcase their instruments and answer questions.

There will also be several social events throughout the week, which spouses and families are welcome to attend. On Monday evening from 5:30 p.m. to 7:30 p.m. ICDD will sponsor an XRD poster session and wine and cheese reception in the Westminster Foyer just outside the exhibition hall. On Tuesday evening from 5:30 p.m. to 7:30 p.m. Chemplex Industries, Inc., will sponsor an XRF poster session and wine and cheese reception in the Westminster Foyer. Finally, on Wednesday evening from 5:30 p.m. to 7:30 p.m. there will be a vendor-sponsored reception held in the exhibit hall.

Other Information

The "Book of Abstracts" will be distributed at the conference on a USB stick again this year, along with a small, printed program booklet as part of the conference's "green" initiative.

Next year's conference will be held at the Big Sky Resort in Big Sky, Montana, from July 28 to August 1, 2014. For more information visit: www.dxcicdd.com ■

Summary

Moxtek® is a leading manufacturer of X-ray windows for low energy X-ray detection. Moxtek manufactures ultra-thin polymer X-ray windows that are attached to metal mounts which house energy dispersive X-ray detectors such as Silicon Drift Detectors (SDDs). These windows allow for transmission of low energy X-rays while maintaining a hermetic seal critical for the X-ray detector's performance. While Moxtek ensures that all windows meet published limits for leak rates, no material is a perfect gas barrier and gasses will diffuse through window assemblies over time. As a continuous improvement effort, Moxtek investigated the effects of plasma cleaning the metal mounts before attaching a window, and achieved around a 40% reduction in the diffusion of helium through the epoxy-to-mount interface.

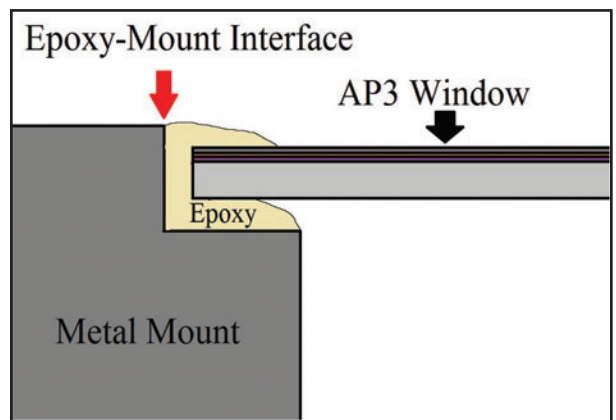


AP3 Window

Methods

Diffusion of helium through Moxtek AP3 window assemblies was measured by using a fixture designed to eliminate the effects of helium diffusing through anything other than the area of interest. Window assemblies were exposed to helium for long periods of time until a steady state diffusion rate was achieved. The epoxy-mount interface was one area identified as a source of diffusion.

Solid metal disks were epoxied into window mounts so that all interfaces with the epoxy would be epoxy-to-metal. Some mounts were plasma cleaned prior to attaching while others were not. All parts were then evacuated on the vacuum side and then exposed on the other side to 1 atm of helium for 10 hours allowing a steady state diffusion to occur. Diffused helium was detected using a helium leak detector.

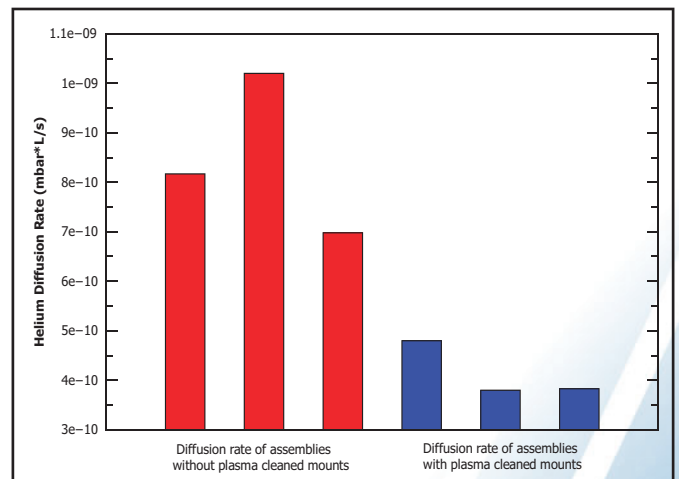


Epoxy-mount diffusion path in AP3 Window

Results / Conclusion

The diffusion rate of helium was measured through the epoxy-to-metal interface of assemblies where metal mounts had been plasma cleaned and metal mounts that were not plasma cleaned. Referencing the figure to the right, the bars in red are the helium steady state diffusion rates of window assemblies whose mounts were only chemically cleaned. The blue bars show the steady state diffusion rates of assemblies whose metal mounts were plasma cleaned prior to attaching the solid metal disks. A 41% average decrease in helium diffusion rate occurred in parts that received a plasma clean from the ones that did not.

Plasma cleaning prior to attaching achieves a better bonding surface that reduces the diffusion of helium, at the epoxy-to-metal interfaces. While no material is a perfect gas barrier, Moxtek is continuously working to improve the hermetic properties of X-ray windows.



Difference in steady state diffusion of helium from mounts that were treated with plasma prior to attaching metal blank and those that were not

To view the complete application note, please visit www.moxtek.com/library



MOXTEK
INNOVATING SOLUTIONS

452 West 1260 North / Orem, UT 84057
Toll Free / 1.800.758.3110
www.moxtek.com
info@moxtek.com

PRODUCT RESOURCES

UV-vis-NIR system

The Cary 7000 Universal Measurement spectrophotometer from Agilent Technologies is designed to provide measurements of transmission, absolute reflection, and scattering without moving the sample.

According to the company, the system is automated and provides 10 absorbance unit capability.

Agilent Technologies,

Santa Clara, CA;

www.agilent.com/chem/cary7000UMS



Agilent Technologies

Energy dispersive spectroscopy detectors

Silicon drift detectors for energy dispersive spectroscopy from Amptek are designed for use with scanning electron microscopes.

According to the company, the low energy response of the detectors extends down to carbon, and the systems are suitable for laboratory and field use and for original equipment manufacturers developing tabletop or handheld XRF analyzers.

Amptek, Inc.,

Bedford, MA;

www.amptek.com



Application note for diesel analysis

An application note from Applied Rigaku Technologies describes the measurement of sulfur in ultralow-sulfur diesel using the company's NEX QC+ high-resolution benchtop EDXRF analyzer. The analysis reportedly complies with standard test method ISO 13032.

Applied Rigaku Technologies,

Austin, TX;

www.rigakuedxrf.com/edxrf/app-notes.html?id=1272_AppNote



Multichannel spectrometers

Multichannel spectrometers from Avantes combine up to 10 spectrometers into one housing in a standard 19-in. rack mount, with the opportunity to combine all into a single output spectrum.

According to the company, the total number of spectrometers connected to a single computer is limited only by USB, memory, or the processor limitations of the host computer.

Avantes,

Broomfield, CO;

www.avantes.com

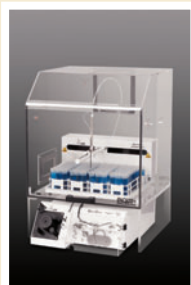


Mercury in groundwater application note

An application note from CETAC Technologies compares two methods for measuring mercury in groundwater: EPA 245.7 and ISO 17852. The note describes how both methods were implemented using the company's QuickTrace M-8000 cold vapor atomic fluorescence analyzer. The results discussed in the publication reportedly indicate more accurate response and lower MDL for the ISO method, attributed to the way the method reduces excess bromine.

CETAC Technologies,

Omaha, NE; www.cetac.com



ICP sample uptake monitor

The TruFlo device from Glass Expansion is designed to digitally and graphically display the sample flow rate to an ICP-OES or ICP-MS nebulizer.

According to the company, an alarm sounds when deviation from specified flow rates occurs, the monitor can be calibrated for a variety of solvents, and the device is available in flow ranges from 0.001 to 4.0 mL/min in both standard and HF-resistant models.

Glass Expansion,

Pocasset, MA; www.geicp.com



Cylindrical and flat optics

Certified cylindrical and flat optics from Hellma are designed with radii ranging from 10 mm to 5 m with sizes up to 1 m. According to the company, flats include wedges, prisms, beam splitters, corner cubes, windows, and mirrors.

Hellma USA, Inc.,

Plainview, NY;

www.hellmausa.com

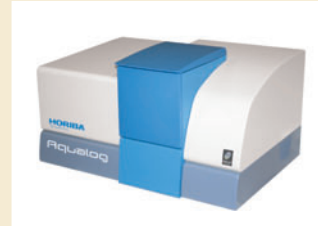


Absorbance and fluorescence system

The Aqualog simultaneous absorbance and fluorescence system from Horiba Scientific is designed to measure colored dissolved organic matter in water 100 times faster than previous fluorescence methods. According to the company, the system offers a lower absorbance and fluorescence excitation wavelengths down to 200 nm and extended emission coverage up to 800 nm.

Horiba Scientific,

Edison, NJ; www.aqualog.com



Database

The PDF-4+ 2013 database from ICDD is designed to provide comprehensive material coverage for inorganic materials with 340,653 entries. According to the company, the database supports automated quantitative analyses by providing key reference data required for these analyses.

ICDD,
Newtown Square, PA;
www.icdd.com



LED sources

Fiber-coupled LED sources from Mightex are designed to combine up to eight LEDs into one fiber with high efficiency without any moving parts in the optical path, with wavelengths ranging from 240 nm to 940 nm. According to the company, the LEDs can be controlled, switched, or dimmed individually or in any combination.

Mightex,
Pleasanton, CA;
www.mightexsystems.com

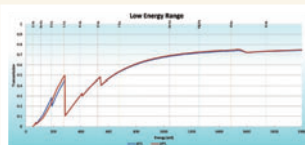


EDS detector windows

The AP5 EDS detector window for light element detection from Moxtek is designed with an ultrathin polymer film to provide maximum transmission of low energy X-rays with zero visible light leaks.

According to the company, the window can be used in applications where light element detection is important and beryllium windows are ineffective.

Moxtek,
Orem, UT.
www.moxtek.com



Handheld Raman spectrometer

The IDRaman mini handheld Raman spectrometer from Ocean Optics is designed for applications ranging from chemical and explosives agent detection in the field to quality assurance and quality control sampling routines in the laboratory. According to the company, the spectrometer measures $3.6 \times 2.8 \times 1.5$ in., weighs 11 oz, and uses two AA batteries.

Ocean Optics,
Dunedin, FL; www.oceanoptics.com



X-ray scattering module

The ScatterX⁷⁸ module from Panalytical is designed to acquire high-quality small- and wide-angle X-ray scattering data in an angular range from 0.08 to 78 degrees. According to the company, the module consists of a vacuum chamber that houses beam collimation elements, a sample capsule, and a beamstop. The module reportedly requires no alignment by the user.

Panalytical,
Westborough, MA;
www.panalytical.com



ATR accessory

The GladiATR accessory from PIKE Technologies is designed with expanded temperature control options. According to the company, the single reflection diamond ATR accessory can be configured for heating up to 300 °C and used for high-temperature kinetic or material degradation studies.

PIKE Technologies,
Madison, WI;
www.piketech.com



Optical parametric oscillator

The Oriá IR optical parametric oscillator from Radiantis is designed as a sealed, hands-free, fully automated femto-second system that provides wavelength coverage with high average power in the near- and mid-IR. According to the company, the oscillator is compatible with standard femtosecond MHz Ti: sapphire oscillators and is suitable for nonlinear microscopy applications where short pulse durations, high beam pointing, and high power stability are required in the IR.

Radiantis,
Barcelona, Spain; www.radiantis.com



Silicon drift detectors

The XRF200i compact silicon drift detectors from SGX Sensortech (MA) are designed for OEM benchtop XRF applications. According to the company, the detectors are available with active areas ranging from 10 mm² to 100 mm².

SGX Sensortech (MA) Ltd.,
High Wycombe, UK;
www.sgxsensortech.com



Knife mills

Retsch's Grindomix GM 300 knife mills are designed for food sample preparation. According to the company, the mills homogenize quantities of up to 4.5 L and process substances with a high water, oil, or fat content as quickly and reliably as dry, soft, medium-hard, and fibrous products.

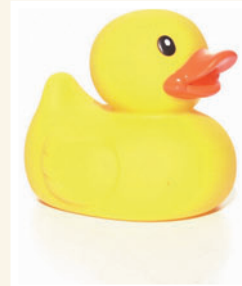
Retsch, Inc.,
Newtown, PA;
www.retsch.com/gm300



PVC and PE solid reference materials

Solid reference materials from SPEX CertiPrep include phthalates in PVC matrix. According to the company, polyethylene standards are also available to customers in the plastics market.

SPEX CertiPrep,
Metuchen, NJ;
www.spexcertiprep.com



Detector

Andor's iDus LDC-DD 416 platform is designed to provide a combination of low dark noise and high QE. According to the company, the detector is suitable for NIR, Raman, and photoluminescence and can reduce acquisition times, removing the need for liquid nitrogen cooling.

Andor Technology,
South Windsor, CT;
www.andor.com



Laboratory-based LIBS analyzers

ChemScan laboratory-based analyzers from TSI are designed to use laser-induced breakdown spectroscopy to provide identification of materials and chemical composition of solids. According to the company, the analyzers are equipped with the company's ChemLytics software.

TSI Incorporated,
St. Paul, MN;
www.tsi.com/ChemScan



Confocal Raman microscope

Horiba Scientific's XploRA One Raman microscope is designed for QA-QC and analytical laboratories in the industrial and routine analytical sectors. According to the company, the microscope's user interface is powered by its Lab-Spec 6 software.

Horiba Scientific,
Edison, NJ;
www.horiba.com/us/en/scientific/marketing-us/xplora-one/



Raman spectrometer

B&W Tek's i-Raman Plus portable Raman spectrometer is designed with a high-efficiency back-thinned CCD detector with deep TE cooling and high dynamic range. According to the company, the spectrometer provides an improved signal-to-noise ratio for up to 30 min of integration time, allowing for measurement of weak Raman signals.

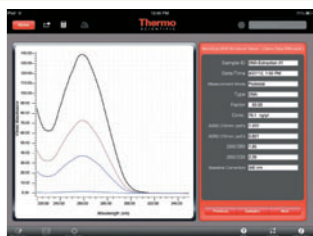
B&W Tek, Newark, DE;
www.bwtek.com/products/i-raman-plus/



Data reviewing and sharing iPad app

The Thermo Scientific NanoDrop user application for iPad is designed to enable users of the company's NanoDrop instruments to take sample data on the go. According to the company, the app allows users to import and view data, and compare concentration, purity, and spectral information.

Thermo Fisher Scientific, San Jose, CA;
www.thermoscientific.com/nanodropapp



EDXRF spectrometer

Shimadzu's EDX-LE energy dispersive X-ray fluorescence spectrometer is designed for screening elements regulated by RoHS/ELV directives. According to the company, the spectrometer is equipped with automated analysis functions and a detector that does not require liquid nitrogen.

Shimadzu Scientific Instruments,
Columbia, MD;
www.ssi.shimadzu.com



Silicon drift detector

EDAX's thermoelectrically cooled 50-mm² silicon drift detector is designed for use in its Orbis micro-XRF elemental analyzer system for high-resolution spectral acquisition. According to the company, the system can be useful for those who make measurements on small fragments, coatings and deposits on thin substrates (such as ink on paper), biological samples, and trace element analysis using heavy filters to improve sensitivity.

EDAX, Mahwah, NJ; www.edax.com



Photovoltaic measurement system

Newport Corporation's Oriol IQE-200 photovoltaic cell measurement system is designed for simultaneous measurement of the external and internal quantum efficiency of solar cells, detectors, and other photon-to-charge converting devices. The system reportedly splits the beam to allow for concurrent measurements. The system includes a light source, a monochromator, and related electronics and software. According to the company, the system can be used for the measurement of silicon-based cells, amorphous and mono/poly crystalline, thin-film cells, copper indium gallium diselenide, and cadmium telluride.

Newport Corporation, Irvine, CA; www.newport.com



Raman analyzers

The ProRaman-L series Raman spectrometers from Enwave Optronics are designed to provide measurement capability down to low parts-per-million levels. According to the company, the instruments are suitable for process analytical method developments and other measurements requiring high sensitivity and high speed analysis.

Enwave Optronics, Inc.,

Irvine, CA;

www.enwaveopt.com

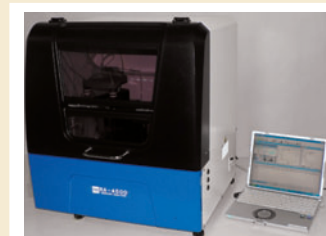


Mercury analyzer

The RA-4500 mercury analyzer from Nippon Instruments is designed to fully automate the sample digestion and analysis for mercury in wastewaters, drinking water, and other aqueous samples. According to the company, features include NIST-traceable temperature logging, a color sensor for potassium permanganate verification, and a built-in exhaust system.

Nippon Instruments North America,

College Station, TX; www.hg-nic.us



LASER-INDUCED BREAKDOWN SPECTROSCOPY FOR THE ANALYTICAL LABORATORY

LIVE WEBINAR: Tuesday, July 23, 2013 at 8:00 am PDT/ 11:00 am EDT

Register Free at www.spectroscopyonline.com/laser

EVENT OVERVIEW:

Laser-Induced breakdown spectroscopy (LIBS) is gaining acceptance as a complement to ICP-OES and other elemental analysis methods. This webcast will illustrate laboratory uses of LIBS that provide both qualitative and quantitative data. Examples from pharmaceutical, metals, and other process industries will show how LIBS direct elemental analysis can save time and provide crucial information from routine analysis to depth profiles and surface concentration maps.

Key Learning Objectives:

- Learn how LIBS analysis provides quantitative elemental concentrations, while avoiding time-consuming digestion steps.
- See how analysts use LIBS as a complement to other methods
- Understand the unique features of the ChemReveal Desktop LIBS system.

Who Should Attend:

- Laboratory analytical chemists
- Core laboratory managers
- Researchers interested in material science, geochemistry
- Quality assurance and inspection professionals for positive material identification (PMI)

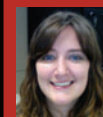


PRESENTER:

Dr. Steve Buckley
Director of Market Development
TSI Incorporated



Dr. Phillip Tan
Sr. Global Product Manager
TSI Incorporated's
ChemLogix Business Unit



MODERATOR:

Meg Evans
Managing Editor
Spectroscopy

Sponsored by



UNDERSTANDING, ACCELERATED

Presented by



For questions, contact **Kristen Farrell** at kfarrell@advanstar.com



ASSUR

THE MOST SENSITIVE HANDHELD RAMAN ANALYZER

- Rapid Analysis to Verify 100% of Incoming Raw Material
- FULL 21 CFR Part 11 Compliant



Enwave Optronics, Inc.

www.enwaveopt.com | sales@enwaveopt.com | Tel: 1-949-955-0258

Spectroscopic

Sampling Supplies / Accessories

NMR • EPR



IR • FTIR



UV • VIS • FL



AA • ICP



Full Catalogs with Pricing
www.newera-spectro.com



New Era Enterprises, Inc.
1-800-821-4667
cs@newera-spectro.com

New Accessory Catalog!



PIKE
TECHNOLOGIES

6125 Cottonwood Drive
Madison, WI 53719
608.274.2721
email: info@piketech.com

www.piketech.com

AVANTES
solutions in spectroscopy

- Spectrometers
- Light Sources
- Fiber Optics

Call for Application Notes

Spectroscopy is planning to publish the next edition of The Application Notebook in September 2013. As always, the publication will include paid position vendor application notes that describe techniques and applications of all forms of spectroscopy that are of immediate interest to users in industry, academia, and government.

If your company is interested in participating in this special supplement, contact:

Michael J. Tessalone, Group Publisher • (732) 346-3016

Edward Fantuzzi, Publisher • (732) 346-3015

or

Stephanie Shaffer, East Coast Sales Manager • (508) 481-5885

Ad Index

ADVERTISER	PG#	ADVERTISER	PG#	ADVERTISER	PG#
Agilent Technologies	3	Glass Expansion	8	Nippon Instruments North America	28
Amptek	5	Hellma Cells, Inc.	40	Ocean Optics, Inc.	17
Andor Technology Ltd.	22	Horiba Scientific	25	Panalytical	33
Applied Rigaku Technologies	21	ICDD	BRC, 27	PerkinElmer Corporation	31
Avantes BV	50	Metrohm USA	CV4	PIKE Technologies	13, 50
B&W Tek, Inc.	37, 43	Mightex Systems	18	Retsch, Inc.	38
CETAC Technologies, Inc.	23	Milestone, Inc.	11	SGX Sensortech (MA) Ltd.	35
EDAX, Inc.	15	Moxtek, Inc.	7, 45	SPIE Optics and Photonics	CV3
Enwave Optronics, Inc.	50	New Era Enterprises, Inc.	50	Thermo Fisher Scientific	CV2
FACSS	41	Newport Corporation	29	TSI Incorporated	39, 49

2013 Optics+ Photonics

For the latest in optical engineering and applications, solar energy, nanotechnology, organic photonics and space optics research

Register Today

www.spie.org/op1

Conferences & Courses

25–29 August 2013

Exhibition

27–29 August 2013

Location

San Diego Convention Center
San Diego, California, USA

www.spie.org/op1

Technologies

- Nanoscience + Engineering
- Solar Energy + Technology
- Organic Photonics + Electronics
- Optical Engineering + Applications



SPIE[®]

Metrohm NIRSystems

Metrohm extends its portfolio to include solutions for Near Infrared Spectroscopy. Metrohm NIRSystems

- offers leading edge NIR technology
- has over 40 years of NIR expertise
- is serviced and supported by Metrohm

www.metrohmusa.com/nirs





Current Trends in

MASS

Spectrometry

July 2013

SUPPLEMENT TO
LCGC North America | LCGC Europe | Spectroscopy

**Using GC-MS to Analyze
Essential Oils in Cedar Leaves**

**Sample Preparation for
MS-Based Proteomics**

UHPLC in Lipidomics

**Comparing Magnetic Sector and TOF
Systems for Environmental Analysis**

ADVANTAR
SCIENTIFIC

To view CTMS Supplement - [Click on here](#)